

PM – 96/19
April 1996

Anomalous thresholds and edge singularities in Electrical Impedance Tomography

Journal of Mathematical Physics, **37**, 4388, (1996)

Sorin Ciulli and Simona Ispas

Laboratoire de Physique–Mathématique, URA 768 du CNRS
Université de Montpellier II, Montpellier, France

Michael Pidcock

Applied Analysis Research Group, School of Computing and Mathematical Sciences
Oxford Brookes University, Oxford, United Kingdom

Abstract: Studies of models of current flow behaviour in Electrical Impedance Tomography (EIT) have shown that the current density distribution varies extremely rapidly near the edge of the electrodes used in the technique. This behaviour imposes severe restrictions on the numerical techniques used in image reconstruction algorithms. In this paper we have considered a simple two dimensional case and we have shown how the theory of end point/pinch singularities which was developed for studying the anomalous thresholds encountered in elementary particle physics can be used to give a complete description of the analytic structure of the current density near to the edge of the electrodes. As a byproduct of this study it was possible to give a complete description of the Riemann sheet manifold of the eigenfunctions of the logarithmic kernel. These methods can be readily extended to other weakly singular kernels.

arXiv:hep-th/9604019v3 23 Aug 1996

I. INTRODUCTION

There are numerous examples of practical situations where electric current is used to probe the interior of some object of interest. One emerging technology which specifically uses this approach has become known as Electrical Impedance Tomography (EIT). This is a method of medical and industrial imaging in which electrical currents are applied to the surface of an object and the induced surface voltage is measured. These data are then used to produce an image of the conductivity distribution in the interior of the object. An extensive literature exists on EIT.¹

The particular feature of EIT which is of interest to us here is related to the observation that in practice the electric current can be applied only through a finite number of electrodes—currently in the range 16–64 for two dimensional applications. The consequences of this fact and the appropriate mathematical modelling of the electrodes have been discussed in a number of papers.^{2–4}

In medical applications one of the significant problems for EIT is the existence of a thin layer of material of high, but unknown, contact impedance lying between the current drive electrodes and the body. Various models have been proposed to describe this phenomenon but one which has strong experimental support⁵ is to suppose that on the (finite size) electrodes the electric potential, Φ , is related to the electric current $\sigma(\partial\Phi/\partial n)$ by

$$\Phi + \mathcal{Z}\sigma\frac{\partial\Phi}{\partial n} = V$$

where σ is the conductivity just below the electrode, \mathcal{Z} is the contact impedance and V is the potential of the electrode (a constant). The induced voltage, Φ , is found by making measurements on high impedance electrodes, also attached to the surface.

This model has been studied numerically using a boundary Fourier technique² for the case of constant \mathcal{Z} and an interesting phenomenon which was observed was the appearance of very sharp peaks in the current density distribution at the edge of the electrodes. More recently the model has been studied numerically for non-constant \mathcal{Z} using the weakly singular integral equation described in Eq. (6) below. Although the singularity is weak, its existence has important consequences for the numerical treatment of this equation. Details of this work will be given elsewhere⁶ but the point which we wish to emphasize here is that the distinctive sharp peak behaviour occurs for a wide range of conductivity distributions and contact impedance forms. In Fig. 1 we show typical results for the current density distribution in the case of eight electrodes with an input current on the l th electrode of $\cos\theta_l$.

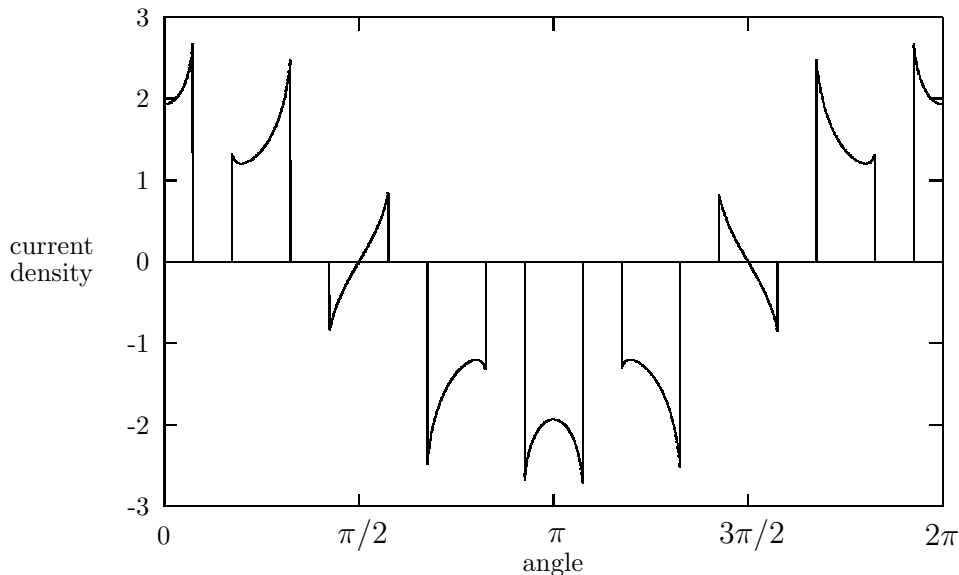


FIG. 1. The current density distribution obtained solving Eq. (6) numerically for the case of 8 electrodes, each having a contact impedance equal to 0.22.

An unwelcome consequence of the sharpness of these peaks is that the direct numerical modelling of the potential with the finite element method has become an excessively substantial task due to the high number of mesh points needed near to the edge of the electrodes in order to accommodate the rapid variation of the normal derivative of the potential. The aim of this article is to give an explicit analytic description of these singularities in a form which should substantially improve the speed of the numerical computation.

Since the appearance of the peaks is a boundary phenomenon which is very little influenced by the actual values of the conductivity σ inside the disk—see the discussion in Section III about the *dominant singular integral equation*—we shall focus our attention on the constant σ case. In this case the governing partial differential equation is Laplace’s equation and our problem becomes one in potential theory. Consequently, we shall study the electrode model defined above for the standard domain of the unit disk. The importance of the unit disk stems from the fact that the potential problem for any simply connected two dimensional domain can be reduced to the unit disk by an appropriate conformal mapping.

In earlier investigations of these peaks it had been shown⁴ that this problem can be solved explicitly in the *zero* contact impedance case ($\mathcal{Z} \equiv 0$), for the case of two electrodes. In this

specific case one finds that near the edge of the electrodes

$$\frac{\partial\Phi}{\partial n} \sim \frac{1}{\sqrt{x}}$$

where x is the distance, along the boundary, from the edge of the electrode. Thus the normal derivative of Φ becomes infinite at the edge of the electrodes. However if the contact impedance \mathcal{Z} is not zero, although $\partial\Phi/\partial n$ still has sharp peaks at the edge of the electrodes (see Fig. 1), it remains finite since both Φ and V are finite and since $\partial\Phi/\partial n \equiv (V - \Phi)/(\mathcal{Z}\sigma)$. This shows that the nature of the singularities in the $\mathcal{Z} \neq 0$ case *cannot* be obtained from that encountered in the soluble $\mathcal{Z} = 0$ model. Thus, in order to have a correct understanding of these singularities some deeper investigations are necessary and this represents the main goal of the present paper.

Overview of the paper

After a short description of the mathematical model in Section II, in Section III we formulate the boundary problem as an integral equation. As shown there the kernel of this integral equation has a weak (logarithmic) singularity, and this has direct consequences for the singularities of the solution near the electrodes edges. We will describe these singularities in terms of an asymptotic series for the potential.

In pursuing this program we shall have to step off the real axis into the neighbouring complex plane. This will be necessary since we will write the solution of the integral equation as an infinite sum of the free term and the eigenfunctions of the weakly singular kernel. As one knows, there are many examples of series uniformly and absolutely convergent on the real axis which cannot be differentiated term by term [for example $\sum_{n=1}^{\infty} \cos(nx)/n^2$ converges uniformly, while the k th derivatives of its terms contain factors of the form n^{k-2} which spoil any convergence], but in deriving asymptotic expressions we will often have to perform this kind of operation. However, in contrast to what happens on a real interval, in the complex plane there exists a marvellous theorem which states that given a sequence $\{f_i\}$ of functions holomorphic in some domain Ω which converge uniformly, $f_i \rightarrow f$, on all compact subsets of Ω , then (a) f is a holomorphic function in Ω and (b), f'_i as well as the higher derivatives $f_i^{(n)}$ tend uniformly towards f' and $f^{(n)}$ on any compact subset of Ω . In some way by walking in the complex plane around the singularity one has a better view of what really happens there.

In studying the analytic properties of the free term (Section IV) and of the eigenfunctions (Section V), we shall use techniques similar to those from the 'pinch and end point singularities

theory' which was developed some time ago by Eden, Landshoff, Olive and Polkinghorne⁷ in elementary particle physics. However our problem is more complex than that related to the Feynman graphs in two respects. First we will have to consider moving cuts rather than moving poles, and second, we will no longer have integrals over some explicitly given functions, but integrals over the *a priori* unknown eigenfunctions whose singularities we are trying to find.

Handling infinite series can also be dangerous because spurious singularities may creep in as happens, for example, with the common geometric series. The proof that this does not happen in the neighbourhood of the singular point is given in the first subsection of the Section V. The analytic properties of the eigenfunctions and the recursive procedure to compute the coefficients in the asymptotic expansions are given in Section V B [see Eq. (67)]. From this expansion it follows that the spikes of the current density near the edge of the electrodes are of the form

$$\frac{\partial\Phi}{\partial n} \sim \sum_{m=1}^r \sum_{k=1}^m c_{mk} x^m \cdot \log^k(x) + \mathcal{O}(x^{r+1-\varepsilon}) + \text{regular part},$$

where x is the distance along the boundary from the edge of the electrode and c_{mk} some real coefficients. Since the derivative of $x \log(x)$ is $1 + \log(x)$, this means that although these spikes are *finite* they have *infinite derivatives*.

II. THE MATHEMATICAL MODEL FOR EIT

The usual model used to describe the forward problem in EIT is obtained by considering the object as consisting of isotropic material with conductivity distribution σ contained in an open, simply connected region Ω surrounded by a reasonably smooth boundary $\partial\Omega$. On the surface, $\partial\Omega$, a number, L , of electrodes are attached and electrical current is applied.

In this case Maxwell's equations give:

$$\nabla \cdot (\sigma \nabla \Phi) = 0 \quad \text{in } \Omega. \quad (1)$$

Further, the total current driven on the l th electrode $I_l = \int_{\Gamma_l} \sigma \partial\Phi / \partial n$ is a known quantity and there is no current outflow outside the region covered by the electrodes, $\Gamma = \Gamma_1 \cup \Gamma_2 \cup \dots \cup \Gamma_L$. If we now introduce our electrode model mentioned earlier to the case when σ is constant and Ω is the unit disk, the physical problem is equivalent to the mathematical problem of solving the following boundary value problem:

$$\nabla^2 \Phi(z) = 0 \quad \text{in } \Omega, \quad (2)$$

$$\begin{aligned}
\frac{\partial\Phi}{\partial n} &= 0 && \text{on } \partial\Omega \setminus \Gamma, \\
\frac{\partial\Phi}{\partial n} &= \frac{1}{\mathcal{Z}_l(z)}[V_l - \Phi(z)] && \text{on the electrode } \Gamma_l \subset \partial\Omega, \\
\int_{\Gamma_l} \frac{\partial\Phi}{\partial n} d\theta &= I_l, && l = 1, \dots, L,
\end{aligned} \tag{3}$$

for constant induced voltage, V_l , and total current driven, I_l , on each electrode. Here \mathcal{Z}_l represents the contact (the 'skin') impedance and $\Phi(z = e^{i\theta} \in \Gamma_l)$ is the potential just underneath 'the skin'.

III. THE INTEGRAL EQUATION

If the values of the normal derivative

$$\left. \frac{\partial\Phi}{\partial n} \right|_{z=e^{i\theta}}$$

were known everywhere on the boundary $\partial\Omega$ of the unit disk, we would be considering a classical Neumann problem, which is readily solved by means of the formula

$$\Phi(z) = \int_0^{2\pi} \mathcal{N}(z, e^{i\theta'}; 0) \left. \frac{\partial\Phi}{\partial n} \right|_{z'=e^{i\theta'}} d\theta' + \text{const.}, \tag{4}$$

where the Neumann kernel $\mathcal{N}(z, z'; 0)$ is

$$\mathcal{N}(z, z'; 0) = -\frac{1}{\pi} \log |z - z'|,$$

with $z' = e^{i\theta'}$ on the unit circle.

If we integrate the kernel with the values of the normal derivative $\partial\Phi/\partial n$ on the unit circle, we obtain a function Φ which is harmonic throughout the unit disk, which vanishes at $z = 0$ and which has the prescribed normal derivative values on the boundary. Similar kernels $\mathcal{N}(z, z'; z_0)$ producing functions vanishing at $z = z_0$ rather than at $z = 0$ can be written easily,⁸ but the knowledge of the normal derivative determines Φ only up to a constant.

For what follows it is interesting to continue the Neumann integral (4) up to the boundary. Since

$$\left| e^{i\theta} - e^{i\theta'} \right|^2 \equiv 2[1 - \cos(\theta' - \theta)],$$

if z and z' are of the form $z = e^{i\theta}$ and $z' = e^{i\theta'}$ the Neumann kernel on the unit circle reads:

$$\begin{aligned}
\mathcal{N}(e^{i\theta}, e^{i\theta'}; 0) &= -\frac{1}{2\pi} \log\{2[1 - \cos(\theta' - \theta)]\}, \\
&= -\frac{1}{\pi} \log \left| 2 \sin \left(\frac{\theta' - \theta}{2} \right) \right|.
\end{aligned} \tag{5}$$

In our case the normal derivative is known explicitly only on that part of the boundary which lies between the electrodes (i.e., on $\partial\Omega \setminus \Gamma$) where $\partial\Phi/\partial n$ is identical to zero. However, since the integral representation (4) can be continued up to the boundary, conditions (3) yield a linear integral equation for the boundary values $\rho(\theta) \equiv \Phi(e^{i\theta})$ of the potential:

$$\rho(\theta) = -\frac{1}{\pi} \sum_{l=1}^L V_l \int_{\Gamma_l} \frac{d\theta'}{\mathcal{Z}_l(\theta')} \log \left| 2 \sin \left(\frac{\theta' - \theta}{2} \right) \right| + \frac{1}{\pi} \sum_{l=1}^L \int_{\Gamma_l} \frac{d\theta'}{\mathcal{Z}_l(\theta')} \log \left| 2 \sin \left(\frac{\theta' - \theta}{2} \right) \right| \rho(\theta'). \quad (6)$$

Although the kernel

$$-\frac{1}{\pi} \log \left| 2 \sin \left(\frac{\theta' - \theta}{2} \right) \right|$$

becomes infinite each time θ' equals θ , this logarithmic singularity is weak enough to be L^2 integrable. The kernel is therefore of Hilbert–Schmidt type and so one can benefit from all the advantages of Fredholm integral equations of the second kind, namely the existence and uniqueness of an L^2 solution $\rho(\theta)$.

Equation (6) may be rewritten in a form which exhibits the logarithmic singularities of the kernel. Taking $e^{i\theta} \in \Gamma_{l_0}$ we may write

$$\begin{aligned} \rho(\theta) &= -\frac{1}{\pi} \sum_{l \neq l_0} \int_{\Gamma_l} \log \left| 2 \sin \left(\frac{\theta' - \theta}{2} \right) \right| \frac{[V_l - \rho(\theta')]}{\mathcal{Z}_l(\theta')} d\theta' - \frac{1}{\pi} \int_{\Gamma_{l_0}} \log \left| \frac{\sin \left(\frac{\theta' - \theta}{2} \right)}{\left(\frac{\theta' - \theta}{2} \right)} \right| \frac{[V_{l_0} - \rho(\theta')]}{\mathcal{Z}_{l_0}(\theta')} d\theta' \\ &\quad - \frac{1}{\pi} V_{l_0} \int_{\Gamma_{l_0}} \frac{d\theta'}{\mathcal{Z}_{l_0}(\theta')} \log |\theta' - \theta| + \frac{1}{\pi} \int_{\Gamma_{l_0}} \frac{d\theta'}{\mathcal{Z}_{l_0}(\theta')} \log |\theta' - \theta| \rho(\theta'). \end{aligned} \quad (7)$$

In order to study the local behaviour of the solution $\rho(\theta)$ near the edges of the l_0 th electrode, we absorb the first two terms which are continuous into the 'free term' of the so called *dominant singular integral equation*,⁹ which is of the form:

$$f(x) = g(x) + \lambda \int_0^1 K(x, t) f(t) dt, \quad 0 \leq x \leq 1, \quad (8)$$

$$K(x, t) \equiv \log |t - x|. \quad (9)$$

Here the points $x = 0$ and $x = 1$ correspond to the edges of the electrode under consideration. Equation (8) can be readily deduced from (7) by a suitable change of variables and functions in the $\mathcal{Z}_l(\theta)$ constant case, but as we shall show elsewhere¹⁰ the discussion for the general case (non-constant \mathcal{Z}_l , non-constant σ) is fairly similar. When we follow this procedure we find that, as well as the first two terms from Eq. (7) which are regular, the function $g(x)$ contains the term

$$-\frac{1}{\pi} V_{l_0} \int_{\Gamma_{l_0}} \frac{d\theta'}{\mathcal{Z}_{l_0}(\theta')} \log |\theta' - \theta|,$$

so that after the changes of variables $g(x)$ has the form

$$g(x) = \int_0^1 \log |t - x| w(t) dt + \text{regular part.}$$

For the convenience of some subsequent proofs we shall also be interested in the iterated equations obtained by replacing $f(t)$ under the integral by the right hand side of the integral equation (8):

$$\begin{aligned} f(x) &= g_2(x) + \lambda^2 \int_0^1 K_2(x, t) f(t) dt, \\ f(x) &= g_3(x) + \lambda^3 \int_0^1 K_3(x, t) f(t) dt, \dots \end{aligned} \tag{10}$$

and so on, where

$$\begin{aligned} g_2(x) &= g(x) + \lambda \int_0^1 K(x, t) g(t) dt, \\ g_3(x) &= g_2(x) + \lambda^2 \int_0^1 K_2(x, t) g(t) dt, \dots \end{aligned} \tag{11}$$

and

$$\begin{aligned} K_2(x, t) &= \int_0^1 K(x, \tau) K(\tau, t) d\tau, \\ K_3(x, t) &= \int_0^1 K_2(x, \tau) K(\tau, t) d\tau, \dots \end{aligned} \tag{12}$$

If this iteration had been continued indefinitely we would have found the Neumann series for f . Since these series usually converge only for very small values of λ , we shall not use them but stop after a finite number of terms and take advantage of the fact that the eigenvalues of $K_j(x, t)$ are the powers $\{\lambda_n^j\}$ of the eigenvalues $\{\lambda_n\}$ of $K(x, t)$. Indeed this will be quite helpful in some subsequent convergence proofs.

IV. SINGULARITY OF THE FREE TERM

In this and in the next section we shall try to find the analytic structure of the edge singularities of the solution without solving the integral equation, the latter being possible only numerically or in some very special cases.⁴ To this aim we shall use methods similar to those from the theory of the pinch or of the end point singularities,⁷ well known to particle physicists working in analytic S-matrix theory. As a preparation to what follows it is probably helpful to look to the corresponding chapters from the classical book of Eden, Landshoff, Olive and Polkinghorne.⁷

In this section we shall deal with the free term $g(x)$ of Eq. (8). As mentioned in the Introduction, in order to find the analytic structure of the singularities we have to step into the neighbouring complex plane. We shall start our investigations with some negative values z_0 of z for which $\log|t-z| = \log(t-z)$ since the integration variable t is between 0 and 1. Having to perform analytic continuations we prefer to handle holomorphic expressions ($\log|t-z|$ is not a holomorphic function of z) and so, instead working with $g(x)$ we shall focus our attention on functions of the kind

$$F(z) = \int_0^1 \log(t-z)w(t)dt \quad (13)$$

where the weight $w(t)$ is a function of t , which is holomorphic (no cuts or other singularities) in neighbourhoods of $t=0$ and $t=1$. Although the holomorphic extension $F(z)$ is different from $g(x)$, it is closely related to it since, up to regular terms, $\text{Re } F(x \pm i\varepsilon) = g(x)$ for $x \in [0, 1]$ and $\varepsilon \searrow 0$. Since the weight $w(t)$ may differ very much from one case to another, integral (13) cannot be performed explicitly. Therefore it will be interesting to have a mathematical procedure which should be able to predict the form of the singularity *without* actually performing the integrals. However, in order to have a partial check of the results which will be obtained below, we note that in the simplest case $w \equiv 1$ we obtain $F_{w \equiv 1}(z) = z \log(-z) + (1-z) \log(1-z) - 1$.

As mentioned at the end of the last section, if λ is small enough the Neumann series converge and so the solution can be written in terms of the free terms g_j of the iterated equations. Therefore at the end of this section we shall discuss briefly the singularity of the iterated functions $g_j(x)$ since they provide a check of the results obtained in Section V in the general case.

A. Different ways of defining a cut

We recall that the features which are important when considering the cut structure of complex functions are the locations of the branch points and not the way in which the cut is taken. Indeed, the cut can be deformed or trailed as will become apparent below, in Figs. 3 to 5. As a first example, consider the function $F_{w \equiv 1}(z)$ given above. To define the cut of the first term $z \log(-z)$, we first introduce the function $Z(z) = -z$ and ask then that the cut of $\log Z(z)$ should run along the positive Z real axis. One achieves this by writing $Z = |Z| \exp(i\phi)$ and requiring ϕ to be in the range $[0, 2\pi)$. With these conditions the cut of the first term, $z \log(-z)$, of $F_{w \equiv 1}(z)$ runs along the negative z real axis. The function $z \log(-z)$ is real and equal to $z \log|-z| \equiv -|z| \log|z|$ below the cut. Above the cut it will contain an additional imaginary

part equal to $2i\pi z$. There will be no cut along the positive z real axis, here the value of $z \log(-z)$ is equal to $z \log|z| + i\pi z$ both above and below the real axis.

It is not compulsory to take the cut of the second term of $F_{w\equiv 1}(z)$ to the left. Indeed, if we define a new variable $Z(z) = 1 - z$, we can redefine the 'fundamental Riemann sheet' of $\log Z$ by requiring that the argument ϕ of Z to be between $-\pi$ and π rather than between 0 and 2π , so that the cut of $\log Z = \log(1 - z)$ will run along the negative real Z axis. Summarising $F_{w\equiv 1}(z)$ has no cut on the interval $[0, 1]$ but two cuts running from $-\infty$ to 0 and from 1 to ∞ .

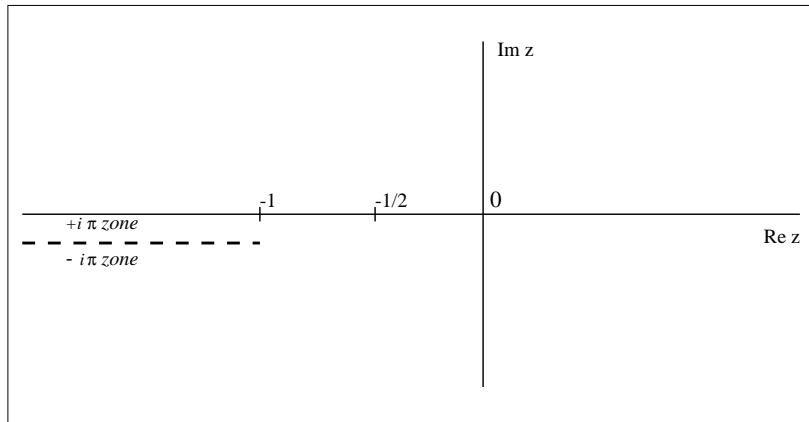


Fig. 2a.

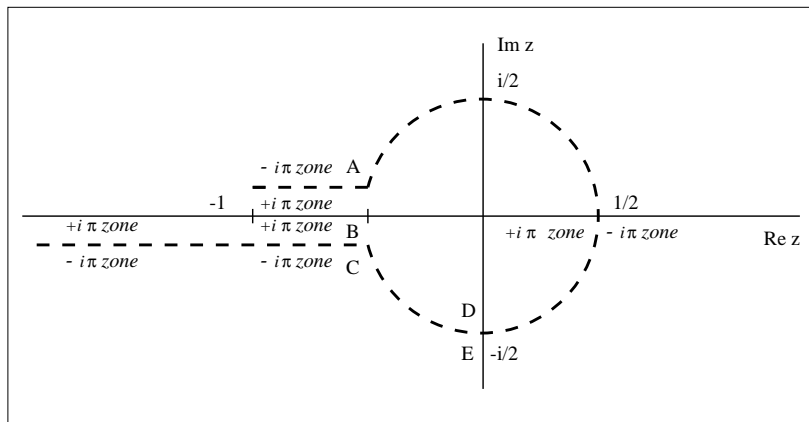


Fig. 2b.

FIGS. 2. Example of two different definitions of the cut of $\log(z + 1)$.

The possible patterns for the cut of the logarithm are not exhausted by the cases discussed above. To have a further example let us consider for instance the function $Z(z) \equiv 1 + z$ and begin with a cut of $\log Z$ running along the negative Z real axis. In this case the cut of $\log(z + 1)$ looks as in Fig. 2a where the $\pm i\pi$ zones mean that the values just above or beneath the cut differ by $\pm i\pi$ from the mean value across the cut. (For illustration purposes we have slightly

deplaced the cut: as it stands it corresponds to the function $\log[z - (-1 - i\varepsilon)]$, $\varepsilon > 0$.)

However we could alternatively define the cuts to run as in Fig. 2b where again the $\pm i\pi$ zones mean that the values of the logarithm differ by $\pm i\pi$ from the mean value across the cut (which is not necessarily real). With these specifications one finds immediately that the value of $\log(z + 1)$ at the points A , B and C are, up to epsilons, equal respectively to $\log|z_A + 1|$, to $\log|z_A + 1| + 2i\pi$ and again to $\log|z_A + 1|$. As a further example, the values of $\log(z + 1)$ at the points $D(z = -i/2 + i\varepsilon)$ and $E(z = -i/2 - i\varepsilon)$ are respectively $\log\sqrt{5/4} - (26.5/180)i\pi + 2i\pi$ and $\log\sqrt{5/4} - (26.5/180)i\pi$, while the mean value across the cut is there equal to $\log\sqrt{5/4} - (26.5/180)i\pi + i\pi$.

B. 'Hooking' the integration contour

Let us come back to the function $F(z)$. In what follows it is important to consider separately the parameter (the 'control') z -plane, and the complex t -plane where the integration is performed. As stated above, our aim is to find the singularities of $F(z)$, in the 'control' z -plane, without performing the integration explicitly. Since our final goal is the description of the singularity of $F(z)$ at $z = 0$, in this section we shall consider only analytic continuations performed in some neighbourhood of the origin. A similar discussion can be made for the other end point $z = 1$.

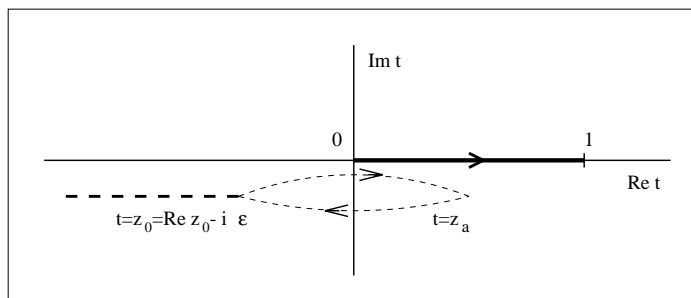


FIG. 3. Integration path (full line) and cut of the logarithm (dashed).

Suppose that initially z lies somewhere immediately below the negative real axis in the complex z -plane: $z = z_0 \equiv x_0 - i\varepsilon$, where $x_0 < 0$ and $\varepsilon > 0$. The function $\log(t - z)$ from the integral of Eq. (13) has, as a function of t (i.e. in the complex t -plane where the integration is performed), a cut running parallel to the real t -axis from $t = -\infty$ to $t = z$ (see the dashed line in Fig. 3). From the point of view of the integration t -space, z is a parameter. Suppose now that z moves towards a point $z_a = x_a - i\varepsilon$ ($x_a > 0$) and then returns to z_0 ($x_0 < 0$) without crossing the integration contour. Correspondingly, the head of the cut of the logarithm (as a function

of t) will move in the t -plane as shown in Fig. 3, but, since it will never cross the integration contour, the value of $F(z_0)$ will be identical with the value that the function $F(z)$ had before the point z began to move from z_0 .

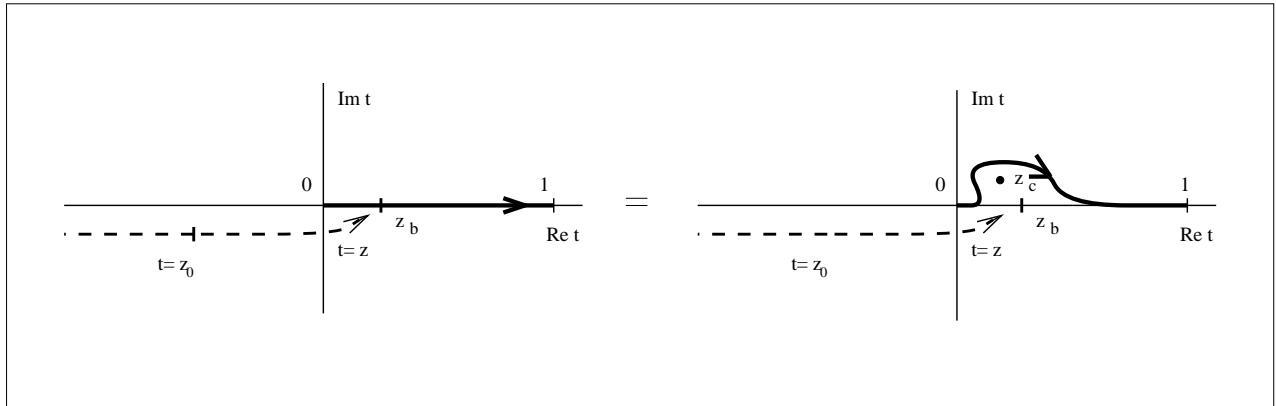


FIG. 4. The integrals over $[0, 1]$ and over the deformed path are identical if $w(t)$ is holomorphic.

The situation is however different if the path followed by the point z in the control complex z -plane crosses the segment $[0, 1]$ before returning to the initial position $z = z_0$. Here again the path followed by the 'head' of the cut begins at z_0 and ends at the same point, but this time it winds around the integration end point $t = 0$, crossing the real axis at $t = z_b$ as shown in Figs. 4 and 5.

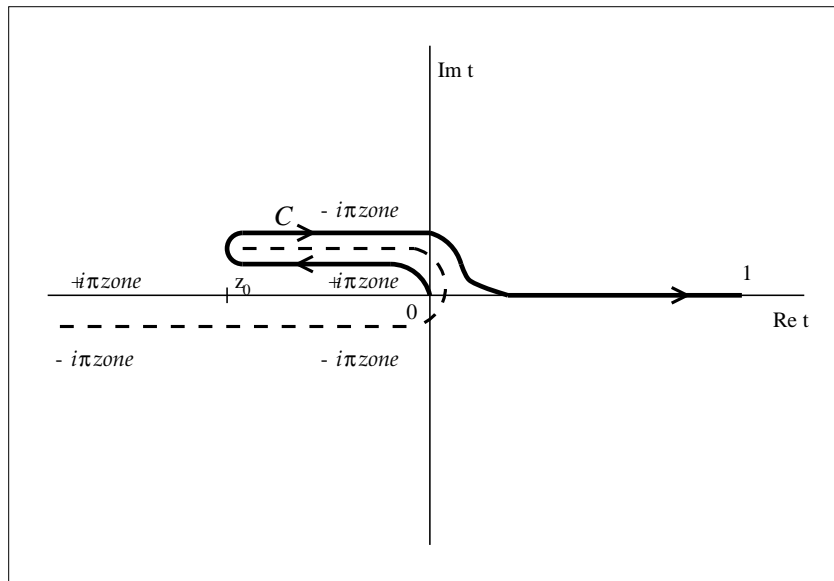


FIG. 5. The moving cut deforms the integration contour and produces an Anomalous Threshold.

A genuine analytic continuation of the function $F(z)$ should, of course, be at least continuous, i.e. have no jumps or other discontinuities. Therefore, even before the end point $t = z$ of

the singularity of the logarithm reaches the point $t = z_b$ which lies on the real axis between 0 and 1, (see Fig. 4), we shall use the freedom we have to deform the integration contours inside the analyticity domain of the integrand without altering in any way the value of the integral $F(z)$.

Since the branch point $t = z$ 'trails' behind it the cut of the logarithm when z moves further through points z_c in the upper half z -plane (Fig. 4) towards z_0 , the value we obtain for the analytic continuation $F^{(1)}(z_0)$ of the initial integral will be given by the integral along the path C in Fig. 5 (the dashed line in Fig. 5 represents the cut of the logarithm; as it stands, the cut ends at the conjugate point $\bar{z}_0 = x_0 + i\varepsilon$ rather than at z_0). Since the value of the logarithm on the lower lip of the emerging part of the cut contains an additional $2\pi i$ with respect to that on the upper lip (recall the discussions about the points A and B from Fig. 2b), the integral on the part of the contour around the cut (see Fig. 5) is

$$\int_0^{z_0} (\log |t - z_0| + 2i\pi) w(t) dt + \int_{z_0}^0 \log |t - z_0| w(t) dt = -2i\pi \int_{z_0}^0 w(t) dt.$$

Here we have supposed that the weight $w(t)$ has no singularities at $z = 0$. Such a point z_0 where the integration starts and which is below the initial integration threshold is called an 'anomalous threshold' in elementary particle physics.

The new value $F^{(1)}(z_0)$ of $F(z)$ obtained by means of this analytic continuation process is hence

$$F^{(1)}(z_0) = 2i\pi \int_0^{z_0} w(t) dt + \int_0^1 \log(t - z_0) w(t) dt \quad (14)$$

where the logarithm has the same determination as in Eq. (13) (i.e. a cut like in Fig. 3).

There are many ways of defining the Riemann sheets of $F(z)$ and here we describe only two of them:

(i) If we now *define* $F(x + iy)$ for any point in the upper half z -complex plane to coincide with the function $F^{(1)}(x + iy)$ defined above, i.e. $F(x + iy) \equiv F^{(1)}(x + iy)$ ($y > 0$), we have implicitly required that the function $F(z)$ should have no cuts on the segment $[0, 1]$ but only on other parts of the real axis. For instance, from the above discussion it follows that along the negative real axis $F(z)$ will have a discontinuity

$$\begin{aligned} \Delta F(x) &= F(x + i\varepsilon) - F(x - i\varepsilon) \equiv F^{(1)}(x + i\varepsilon) - F(x - i\varepsilon) \\ &= 2i\pi \int_0^x w(t) dt, \quad x \in \text{negative real axis}, \end{aligned} \quad (15)$$

which means that $F(z)$ has indeed a cut along the negative real axis. This definition of the 'fundamental' Riemann sheet of $F(z)$ coincides with that for the simple example of $F_{w \equiv 1}(z)$ discussed in the previous subsection.

(ii) Alternatively, we could have required that the function $F(z)$ should have no cuts along the negative real axis. This amounts to redefining its 'fundamental' Riemann sheet: we start again from our $z_0 \equiv x_0 - i\varepsilon$ with $x_0 < 0$, ask that $F^{(0)}(z_0) \equiv F(z_0)$ but then require that the values of $F^{(0)}(z)$ above the real axis should merge, for $\text{Re } z < 0$, with those below the axis. We, therefore, *define* $F^{(0)}(z)$ for $\text{Re } z < 0$ as

$$F^{(0)}(z) = \int_0^1 \log(t - z)w(t)dt. \quad (16)$$

This definition which initially has been given only for $\text{Re } z < 0$ may then be extended to the whole complex plane cut along the real segment $[0, 1]$ (and further, along the positive real axis up to infinity; but, as mentioned at the beginning of this subsection, in order to keep the discussion simple we shall not consider what happens beyond the end point $z = 1$). According to the definition (ii), the function $F^{(0)}(z)$ will have no cuts along the real negative axis, but in return, will have different values along the upper and the lower lip of the real segment $[0, 1]$. In the lower half plane $F^{(0)}(z)$ coincides with the function $F(z)$ corresponding to the previous definition (i) of the fundamental Riemann sheet, but not any longer for $\text{Im } z > 0$ where $F(z)$ was identical to $F^{(1)}(z)$. However, since by the construction of the function $F^{(1)}(z)$ [see the discussion preceding Eq. (14)] we had

$$F^{(0)}(x - i\varepsilon) = F^{(1)}(x + i\varepsilon) + \mathcal{O}(\varepsilon), \text{ for } \varepsilon > 0 \text{ and } 0 < x < 1, \quad (17)$$

it follows that $F^{(1)}(z)$ represents now the analytic continuation of $F^{(0)}(z)$ on the next Riemann sheet—call it sheet (1)—when one crosses the segment $[0, 1]$ in the *upward* direction.

On the other hand, starting from the values $F^{(0)}(x + i\varepsilon)$ from the upper lip of the segment $[0, 1]$ and continuing them *downwards*, one gets the function $F^{(-1)}(z)$:

$$F^{(-1)}(x - i\varepsilon) = F^{(0)}(x + i\varepsilon) + \mathcal{O}(\varepsilon), \text{ for } \varepsilon > 0 \text{ and } 0 < x < 1 \quad (18)$$

which is obtained by deforming the integration contour in the lower half plane. Hence, $F^{(-1)}(z)$ will have the form

$$F^{(-1)}(z_0) = -2i\pi \int_0^{z_0} w(t)dt + \int_0^1 \log(t - z_0)w(t)dt \quad (19)$$

where, again, the logarithm has the same determination as in Eqs. (13) and (16). Further, we see that the jump of $F^{(0)}$ across the cut $[0, 1]$ is

$$\Delta F^{(0)}(x) = -2i\pi \int_0^x w(t)dt, \quad \text{for } 0 < x < 1.$$

The functions $F^{(-1)}$, $F^{(0)}$, $F^{(1)}$ living on the Riemann sheets (-1) , (0) , (1) represent in fact an unique analytic function " $F(z)$ ", the various branches $F^{(-1)}(z)$, $F^{(0)}(z)$, $F^{(1)}(z)$ being nothing but its values on a cutting up of the initial Riemann manifold along some arbitrarily given cuts.

If the function w is holomorphic in some neighbourhood of the origin it admits there an expansion of the form

$$w(t) = a_0 + a_1t + a_2t^2 + \dots, \tag{20}$$

and so, from Eq. (15) we find

$$\Delta F(x) = 2i\pi \left[a_0x + \frac{a_1}{2}x^2 + \frac{a_2}{3}x^3 + \dots \right]. \tag{21}$$

A function which has precisely the same jump along the negative axis is given by

$$\left[a_0 + \frac{a_1}{2}z + \frac{a_2}{3}z^2 + \dots \right] z \log z \tag{22}$$

which provides a mathematically correct and at the same time extremely simple description of the singularity of $F(z)$ near the point $z = 0$.

Before closing this section we shall discuss briefly the structure of the singularities at the origin of the free terms $g_2(z)$, $g_3(z)$, \dots , $g_j(z)$ of the iterated equations (10). In contrast to $g(z)$, these functions are written as integrals of the form (13) over weights $w(t)$ which are no longer holomorphic but contain the singularities of $g(z)$, $g_2(z)$, \dots , $g_{j-1}(z)$ respectively. By straightforward integration we find that the general term of the iterated function $g_j(z)$ is

$$z^m \log^k(z), \quad \text{with } k = 0, 1, \dots, j \text{ and } m \geq k. \tag{23}$$

At this stage we may wonder whether the left hand cuts of the powers of $\log(t)$ appearing under the integrals will not interfere with the above analytic continuation process. This does not occur since the real part of t becomes negative only along the loop in Fig. 5 around the emerging part of the cut of $\log(t - z)$ which is always at the same side of the negative real axis, i.e. always in the same '+ $i\pi$ zone' of the function $\log(t)$. This means that

$$\Delta \left[\int_0^1 \log(t - z) t^m \log^k(t) dt \right] = 2i\pi \int_0^z t^m (\log |t| + i\pi)^k dt, \quad z \in \text{negative real axis.} \tag{24}$$

V. SINGULARITIES OF THE SOLUTION OF THE FULL EQUATION

As mentioned in the Introduction, the specific difficulties of our problem are twofold. We have first to handle moving cuts; this question has been largely discussed in the previous section devoted to the free term. Second—and this is probably the main difference with respect to the classical papers on pinch and end point singularities—we will have to cope with the fact that the singularities of the function under the integral are *a priori* unknown, this function being the solution of the integral equation whose analytic properties we are trying to establish. In this section we shall address this second problem by solving it first for the eigenfunctions which are the natural building blocks of the solution, with the hope that their analytic properties (together with those of the free term) will be transmitted to the solution itself. Of course, this is not at all obvious since we will deal with infinite series and so new singularities may creep in. Therefore before we embark in Section V B on the study of the Riemann sheet structure and the asymptotic expansion of the eigenfunctions, we will first make sure in subsection V A that the analytic properties of the eigenfunctions do exhaust the holomorphic characteristics of the solution. This is probably not entirely pedagogical, but reflects fairly well the way in which our work progressed. We shall have often to refer in Section V A to various analytic properties of the eigenfunctions which will be proved only later in Section V B.

This type of analysis presented here is not restricted to this particular integral equation, but we hope that it provides a working example of how one could proceed in problems involving other kinds of weakly singular kernels. To this end we tried to avoid as much as possible any special properties of the logarithmic kernel—for instance the fact that its null-space $\ker \mathbf{K}$ is empty—and show how we can proceed in the general case. At a first reading or if not particularly interested in these mathematical proofs but only in the practical aspects of the asymptotic expansion, the reader may read only Section V A 1, skip the remainder of the Section V A and pass directly to Section V B.

A. The absence of summation singularities

We shall proceed in a number of stages:

In Section V A 1 we discuss the role of eigenfunction expansions in describing the generic singularities of the solution. In both Sections V A 1 and V A 2 we recall some facts from the theory of integral equations and we identify a class of functions $\{\psi\}$ which can be expanded in terms of the eigenfunctions. We discuss also the possible appearance of additional singularities

due to problems of convergence of infinite sums of functions.

The convergence proofs are provided in two separate subsections. In Section *V A 3* we discuss the continuity of these ψ -functions on the real segment $[0, 1]$ and we show that their eigenfunction expansions converge uniformly there. However, in order to be able to consider the holomorphic properties of the solution $f(z)$ we need a number of results in the complex z -plane. These are derived in Section *V A 4* where, in particular, we prove that no additional singularities appear as a result of the summation of the series. The convergence of the asymptotic parts of the eigenfunctions is discussed in *V A 5*.

1. Generic singularities and eigenfunction expansions

When discussing the possible singularities of the solution of an integral equation we are faced with an apparent paradox. Independently of the specific form of the integral kernel, we may always proceed as a numerical analyst usually does when checking the correctness of computer code: start in the right hand side of Eq. (8) with some 'nice' function $f(t)$ which has no singularities, integrate it with the kernel and then choose the free term $g(x)$ to recover the initial function $f(x)$. So, irrespective of the (integrable) singularities of the kernel, the solution $f(x)$ might be a polynomial, a simple trigonometric function or anything else. One may feel that this type of solution is quite exceptional but this example is enough to show that one *cannot* speak about 'the general singularity' of the solution of an integral equation with a given singular kernel. However one is fully entitled to ask oneself what may happen in the non-exceptional situations, i.e. in the *generic* case.

To this end it is enlightening to express the solution of the integral equation (8) for our logarithmic kernel in terms of the eigenfunctions $u_n(x)$ of $K(x, t)$, defined by

$$u_n(x) = \lambda_n \int_0^1 K(x, t) u_n(t) dt, \quad \text{with } K(x, t) \equiv \log |t - x|, \quad (25)$$

as the series

$$f(x) = g(x) + \sum_{n=0}^{\infty} \frac{\lambda}{\lambda_n - \lambda} g_n u_n(x), \quad (26)$$

derived below in Section *V A 2*, where

$$g_n \stackrel{\text{def}}{=} \int_0^1 g(x) u_n(x) dx. \quad (27)$$

From expansion (26) it is obvious that in the *generic* case when small changes in the form of the function $g(x)$ and hence in $\{g_n\}$ are allowed, both the singularities of the free term $g(x)$

and of the eigenfunctions $u_n(x)$ will appear in the solution $f(x)$ since they will no longer cancel identically.

2. The functions $\psi(x)$

In what follows we shall use systematically the notation $\psi(x)$ for the functions from the range $\text{Ran } \mathbf{K}$ of the integral operator. The properties of these functions are used in the derivation of expansion (26) which plays a central role for the analytic properties of f as a superposition of those of g and of the u_n . However we should exercise great care at this point since additional singularities may creep in. We should have in mind the case of the sequence of functions $1, 1 + z, 1 + z + z^2, \dots$. In the open unit disk this sequence tends to the function $1/(1 - z)$ which has a pole at $z = 1$, whereas all the functions in the sequence are holomorphic in an arbitrary large disk. Later in Section V A 4 we will use a theorem of Vitali and/or of Morera to prove that no additional singularities appear in a neighbourhood of the origin. The theorem of Vitali, for instance, is partially based on the requirement that the elements of the sequence of partial sums should be uniformly bounded, which is clearly not valid in the counter-example with the geometric series if $|z| \geq 1$. Hence we have to make sure that in our case all the requirements of these theorems are fulfilled.

In order to obtain Eq. (26) we first multiply the integral equation (8) by an eigenfunction $u_n(x)$, integrate over the variable x and use the symmetry of the kernel to get

$$f_n = g_n + \frac{\lambda}{\lambda_n} f_n, \quad (28)$$

where the coefficients f_n are defined from $f(x)$ by integrals similar to those in Eq. (27).

From Eq. (28) we find $f_n = \lambda_n g_n / (\lambda_n - \lambda)$, but we should avoid expressing the solution $f(x)$ as a sum $\sum f_n u_n(x)$ since the latter might not converge pointwise and/or the eigenfunctions $\{u_n\}$ might not represent a complete system of orthonormal functions. In the special case of the logarithmic kernel (25) it happens (see Appendix) that the $\{u_n\}$ do represent such a complete orthonormal system, but for an arbitrary kernel K , $\ker \mathbf{K}$ is not empty and so they do not.

Many of the textbook theorems concerning expansions of the type (26) rely on the continuity of the kernel in the square $[0, 1] \times [0, 1]$. Since this is certainly not the case for our logarithmic kernel, some supplementary work is necessary to adapt the proofs to our specific conditions. In the simple cases where the kernel is continuous one usually takes advantage of this fact to prove

that for any square integrable—even singular—function $\varphi(t)$, the function

$$\psi(x) \stackrel{\text{def}}{=} \int_0^1 K(x,t)\varphi(t)dt \quad (29)$$

from $\text{Ran } \mathbf{K}$ is (a) continuous for $x \in [0, 1]$, and (b) expressible in the form of an uniformly convergent expansion

$$\begin{aligned} \psi(x) &= \sum_{n=0}^{\infty} \psi_n u_n(x), \\ &\equiv \sum_{n=0}^{\infty} \varphi_n / \lambda_n u_n(x) \end{aligned} \quad (30)$$

where ψ_n and φ_n are defined by

$$\psi_n = \int_0^1 \psi(t)u_n(t)dt, \quad \varphi_n = \int_0^1 \varphi(t)u_n(t)dt.$$

Here the relation which connects the coefficients ψ_n and φ_n can be obtained by multiplying Eq. (29) by $u_n(x)$, integrating and using the symmetry of the kernel

$$\psi_n = \varphi_n / \lambda_n. \quad (31)$$

The solution $f(x)$ itself does not in general have a representation of the ψ -kind (29), but it is clear from the integral equation (8) that the difference $f(x) - g(x)$ is a true ψ -kind function. Hence it can be expanded as the sum $\sum (f_n - g_n)u_n(x)$, which in turn, using the relation (28) between f_n and g_n , yields the representation (26) for the solution of the integral equation in terms of the free term $g(x)$ and of the eigenfunctions $u_n(x)$.

In Section V A 3 we shall prove that the properties (a) and (b) and hence the expandibility of $f(x) - g(x)$ are also valid in the case of the logarithmic kernel. Before showing that let us notice that if $\ker \mathbf{K}$ is empty as is the case—see the Appendix—with the logarithmic kernel, or if φ is chosen from the orthogonal complement $\ker^\perp \mathbf{K}$ of $\ker \mathbf{K}$, we also have

$$\left\| \varphi(x) - \sum_{n=0}^{\infty} \varphi_n u_n(x) \right\|_{L^2} = 0. \quad (32)$$

However, in contrast with what happens with the ψ -kind functions, Eq. (32) represents only a convergence in the mean, i.e. $\varphi(x)$ does not have, in general, an expansion of the form (30) which converges uniformly. For the study of the analytic properties of the solution we shall need finer properties than those offered by L^2 -space arguments, since, for instance, holomorphy

and uniform convergence of the partial sums are essential for the Morera theorem to be used in Section V A 4.

3. Continuity of $\psi(x)$ in the logarithmic case and the uniform convergence of the $\psi^{(j)}(x)$ on the segment $[0,1]$

This subsection deals with the properties of the ψ -kind functions (29) on the segment $[0, 1]$ for the logarithmic kernel (9). The arguments are quite similar to those which are used in the case of the continuous kernels, but we shall discuss them briefly here as a preparation for the next subsection and as well as to make this paper self contained.

Our logarithmic kernel becomes infinite each time the integration variable t equals x . However, the continuity (a) of $\psi(x)$ on the interval $[0, 1]$ (including at its end points) can be proved in a straightforward manner using the Schwarz inequality. Indeed, for any L^2 function $\|\varphi\|_{L^2} \leq M$ and for any points x and $x + \delta$ belonging to the (closed) segment $[0, 1]$, we have

$$|\psi(x + \delta) - \psi(x)|^2 \leq \int_0^1 [\log |t - (x + \delta)| - \log |t - x|]^2 dt \times M^2 \quad (33)$$

where the integral $\int_0^1 |\varphi(t)|^2 dt$ has been replaced by the bound on the L^2 -norm. If δ is small enough, it can be shown that the integral on the right hand side of (33) can be made smaller than any given nonzero ε^2/M^2 , which proves the continuity of all the ψ -kind functions of the form (29). Since the eigenfunctions $u_n(x)$ by their very definition (25) are also functions of the ψ -kind, we have hence implicitly proved their continuity on the segment $[0, 1]$, including at the end points $x = 0$ and $x = 1$.

We shall now show, (b), that for $x \in [0, 1]$ the finite sums

$$\psi^{(j)}(x) = \sum_{n=0}^j \psi_n u_n(x) \quad (34)$$

converge uniformly to the function $\psi(x)$ defined in Eq. (29).

To this end we shall show first that the functions $\psi^{(j)}(x)$ converge uniformly to some (continuous) function $\psi^{(\infty)}(x)$: a similar proof may be used then for the uniform convergence of the analytic extensions $\Psi^{(j)}(z)$ which will be introduced in the next subsection. From Eq. (31) and from the definition (25) of the eigenfunctions $\{u_n(x)\}$ we have

$$\left| \sum_{j+1}^{j+k} \psi_n u_n(x) \right|^2 \equiv \left| \sum_{j+1}^{j+k} \frac{\varphi_n}{\lambda_n} \cdot \lambda_n \int_0^1 K(x, t) u_n(t) dt \right|^2 = \left| \int_0^1 K(x, t) \sum_{j+1}^{j+k} \varphi_n u_n(t) dt \right|^2,$$

which, using the Schwarz inequality and the fact that the basis $\{u_n(t)\}$ is orthonormal, yields:

$$\left| \sum_{j+1}^{j+k} \psi_n u_n(x) \right|^2 \leq \int_0^1 |K(x, t)|^2 dt \cdot \int_0^1 \left| \sum_{j+1}^{j+k} \varphi_n u_n(t) \right|^2 dt = \int_0^1 |K(x, t)|^2 dt \cdot \sum_{j+1}^{j+k} \varphi_n^2. \quad (35)$$

For each fixed value of x , $0 \leq x \leq 1$, the kernel $K(x, t) \equiv \log |t - x|$ regarded as a function of t is in $L^2[0, 1]$, and so,

$$\int_0^1 K^2(x, t) dt < M^2 < \infty.$$

Since the function φ is also in L^2 , $\sum_{j+1}^{j+k} \varphi_n^2$ tends to zero for $\forall k$ as j increases. Hence the right hand side of (35) can be made arbitrarily small irrespective of the value of x . This means that the sequence $\psi^{(j)}(x)$ converges *uniformly* to some limit $\psi^{(\infty)}(x)$. Now from the continuity of the eigenfunctions $\{u_n(x)\}$ which we have proved above, it follows that the finite combinations $\{\psi^{(j)}(x)\}$ are continuous. Since the $\{\psi^{(j)}(x)\}$ converge *uniformly*, the limit $\psi^{(\infty)}(x)$ is also continuous.

On the other hand, by projecting the kernel onto the basis $\{u_n\}$ we obtain 'the coefficients' $u_n(x)/\lambda_n$. Bessel's inequality then ensures that any sum over the $u_n^2(x)/\lambda_n^2$ is bounded:

$$\sum_{n=0}^{\infty} \frac{u_n^2(x)}{\lambda_n^2} \leq \int_0^1 K^2(x, t) dt (< \infty). \quad (36)$$

Integrating with respect to x we see that $\sum 1/\lambda_n^2$ must also converge and hence the $|\lambda_n|$ must tend to infinity with n . This fact will help us to prove that $\psi^{(\infty)}(x)$ is in fact identical to the function $\psi(x)$ defined in Eq. (29).

Indeed, since both functions $\psi(x)$ and $\psi^{(\infty)}(x)$ are continuous, it is enough to show that the L^2 -norm of their difference is zero. To this end we notice that the difference between $\psi(x)$ and the functions $\psi^{(j)}(x)$ can be written as

$$\psi(x) - \psi^{(j)}(x) = \int_0^1 K^{(j+1)}(x, t) \varphi(t) dt \quad (37)$$

where $K^{(j+1)}(x, t)$ is the truncated kernel

$$K^{(j+1)}(x, t) = K(x, t) - \sum_{n=0}^j \frac{u_n(x) u_n(t)}{\lambda_n}, \quad (38)$$

where we have supposed that the eigenvalues have been labelled according their increasing moduli: $|\lambda_0| \leq |\lambda_1| \leq \dots$. Unlike the procedure followed before, we shall not try to use the Schwarz inequality to prove directly the pointwise convergence of the $\psi^{(j)}(x)$, but we shall go

instead through L^2 -space arguments. Since the first $j + 1$ eigenfunctions $u_0(x)$, $u_1(x)$, \dots , $u_j(x)$ are all in the null space $\ker \mathbf{K}^{(j+1)}$ of the truncated kernel (38), it follows that its eigenvalue with smallest absolute value is λ_{j+1} . If we denote by $K_2^{(j+1)}(x, y)$ the iterated truncated kernel

$$K_2^{(j+1)}(x, y) = \int K^{(j+1)}(x, t)K^{(j+1)}(t, y)dt, \quad (39)$$

its smallest eigenvalue μ will be λ_{j+1}^2 . However for any symmetric Hilbert–Schmidt kernel $\mathcal{K}(x, y)$ we have

$$\sup_{\|\varphi\|=M} \left| \iint \mathcal{K}(x, y)\varphi(x)\varphi(y)dxdy \right| = \frac{M^2}{|\mu|}$$

where μ is the smallest eigenvalue of \mathcal{K} . Hence, taking the integral over the square of the modulus of the left hand side of Eq. (37) we obtain

$$\|\psi - \psi^{(j)}\|_{L^2}^2 = \left| \iint K_2^{(j+1)}(x, y)\varphi(x)\varphi(y)dxdy \right| \leq \frac{M^2}{\lambda_{j+1}^2} \quad (40)$$

which means that $\|\psi - \psi^{(j)}\|_{L^2} \leq M/|\lambda_{j+1}|$. Since $1/|\lambda_{j+1}|$ tends to zero as j increases, so does $\|\psi - \psi^{(j)}\|_{L^2}$. Now, from the uniform convergence $\|\psi^{(j)} - \psi^{(\infty)}\|_{L(\infty)} \rightarrow 0$ which has proved above [see Eq. (35)], we have immediately also the L^2 convergence

$$\|\psi^{(j)} - \psi^{(\infty)}\|_{L^2} \rightarrow 0. \quad (41)$$

From the triangle inequality we have

$$\|\psi - \psi^{(\infty)}\|_{L^2} \leq \|\psi - \psi^{(j)}\|_{L^2} + \|\psi^{(j)} - \psi^{(\infty)}\|_{L^2}, \quad (42)$$

where from Eqs. (40) and (41) we see that the left hand side, which is independent of j , can be made arbitrarily small by a suitable choice of j in the right hand side. This means that $\|\psi - \psi^{(\infty)}\|_{L^2} \equiv 0$ which, since both $\psi(x)$ and $\psi^{(\infty)}(x)$ are continuous, proves that the two functions are identical.

4. The functions $\Psi^{(j)}(z)$ and the theorems of Morera and Vitali

In order to be able to study the nature of the singularities of the functions of ψ -kind, we will have to step off the real axis into the complex z -plane. We shall be particularly interested in the complex plane singularities and the asymptotic expansions near $z = 0$ of eigenfunction expansions of the form (26), related to the solution $f(x)$ of the integral equation. To this end we shall need to know some analytic properties of the eigenfunctions $\{u_n\}$. These will be derived

in Section V B where, similarly to the function $F^{(0)}(z)$ [see Eq. (16) from Section IV], we shall define the analytic functions

$$U_n^{(0)}(z) \stackrel{\text{def}}{=} \lambda_n \int_0^1 \log(t-z) u_n(t) dt, \quad n = 1, 2, 3, \dots \quad (43)$$

Although these functions do not yet represent the analytic continuation of the eigenfunctions $u_n(x)$ which are defined on the real segment $[0, 1]$, they are closely related to them. This specific choice is based, as for $F^{(0)}(z)$, on the fact that for real negative z we have $\log(t-z) \equiv \log|t-z|$, since the integration variable t on the right hand side of Eq. (43) is always between 0 and 1. In contrast to the function $\log|t-z|$ (which is *not* holomorphic because of the modulus), the function $\log(t-z)$ can be extended analytically in the whole (cut) complex z -plane.

As will become apparent in Section V B, the analytic functions $U_n^{(0)}(z)$, $U_n^{(1)}(z)$, $U_n^{(-1)}(z)$, \dots which are the analogues of the functions $F^{(0)}(z)$, $F^{(1)}(z)$, $F^{(-1)}(z)$, \dots , defined in Eqs. (16), (14) and (19), have an infinite Riemann sheet structure; the superscript in parantheses indicates the Riemann sheet under consideration. From the definition of the Riemann sheets and the continuity properties across the cut, we have, similar to Eqs.(17)–(18), for any x real between 0 and 1:

$$U_n^{(k)}(x+i\varepsilon) = U_n^{(k-1)}(x-i\varepsilon) + \mathcal{O}(\varepsilon), \quad \varepsilon > 0, \quad x \in [0, 1]. \quad (44)$$

As will be shown in Section V B 3, the eigenfunctions $u_n(x)$ defined on the interval $[0, 1]$ can be written as simple combinations of the boundary values of $U_n^{(0)}(z)$, $U_n^{(1)}(z)$ and $U_n^{(-1)}(z)$ on the upper and lower lips of the cut:

$$\begin{aligned} u_n(x) &= \frac{1}{2}(U_n^{(0)}(x+i\varepsilon) + U_n^{(1)}(x+i\varepsilon)), \quad \varepsilon \searrow 0, \quad 0 < x < 1, \\ u_n(x) &= \frac{1}{2}(U_n^{(0)}(x-i\varepsilon) + U_n^{(-1)}(x-i\varepsilon)), \quad \varepsilon \searrow 0, \quad 0 < x < 1. \end{aligned} \quad (45)$$

Hence, in analogy with the function $\psi(x)$ and the finite sums $\psi^{(j)}(x)$ defined in the previous subsection for $x \in [0, 1]$, we shall define now for z in some given region Ω of the complex plane, the holomorphic functions

$$\Psi(z) \stackrel{\text{def}}{=} \int_0^1 \log(t-z) \varphi(t) dt, \quad \varphi \in L^2[0, 1], \quad (46)$$

$$\Psi^{(j)}(z) \stackrel{\text{def}}{=} \sum_{n=0}^j \psi_n U_n^{(0)}(z) \equiv \sum_{n=0}^j \frac{\varphi_n}{\lambda_n} U_n^{(0)}(z). \quad (47)$$

Since we are mainly interested in the behaviour of the solution near the origin, it is sufficient to take the region Ω to be the (open) unit disk cut along the real segment $[0, 1]$ (see Fig. 6), but

any other (cut) disk of radius R is also acceptable. The holomorphy of $\Psi(z)$ in Ω follows from the theorem of Morera which states that iff ^{11,12} the function $\Psi(z)$ is *continuous* in the open set Ω and iff

$$\int_{\partial\Delta} \Psi(z)dz = 0 \tag{48}$$

along the border of *every* closed triangle $\Delta \subset \Omega$, (i.e. along any reasonable regular closed contour), then the function $\Psi(z)$ is *holomorphic* in Ω . It is clear that these two conditions are met by any function having the representation (46) for $z \in \Omega$. The continuity of $\Psi(z)$ can be established in a similar way to that of the functions $\psi(x)$ [see Eq. (33)], while the vanishing of the integrals (48) follows—after the interchange of the integral over $t \in [0, 1]$ and integrals in the z -complex plane—from the holomorphy of $\log(t-z)$ as a function of $z \in \Omega$. The theorem of Fubini¹¹ permits this interchange of the integration order since the function $F(z, t) \equiv \log(t-z)\varphi(t)$ is in $L^1[\partial\Delta \times [0, 1]]$ we are interested in. The holomorphy of the functions $\Psi^{(j)}(z)$ is an immediate consequence of the fact that they are finite sums of holomorphic functions.

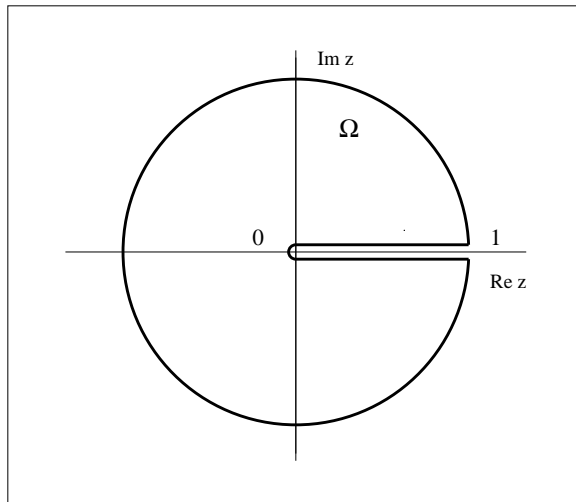


FIG. 6. The open set Ω .

We denote by $\Psi^\infty(z)$ the limit of the sequence $\{\Psi^{(j)}(z)\}$ wherever this limit exists. We will show that *there are no new singularities* which enter the region Ω as a result of the summation process, i.e. that the limit $\Psi^\infty(z)$ is holomorphic in Ω . This is an important point: remind the counterexample with the geometric series discussed at the beginning of the Section *V A 2*.

In studying the analytic properties of the function $\Psi^\infty(z)$, the crucial property is again the uniform convergence—to be proved below—of the sequence $\{\Psi^{(j)}(z)\}$. This might seem surprising since on the real line there exist examples of sequences of infinitely differentiable functions which converge uniformly to functions which are nowhere differentiable. However, in

the complex plane the uniform convergence of the sequences can be used in conjunction with the theorem of Morera to prove the holomorphy of their limits. Indeed, as a first consequence of the uniform convergence of the sequence $\{\Psi^{(j)}(z)\}$ one obtains the continuity of its limit $\Psi^\infty(z)$. Secondly, the identity

$$\int_{\partial\Delta} \Psi^\infty(z) dz = 0 \quad (49)$$

follows from the vanishing of the corresponding integrals over the holomorphic functions $\Psi^{(j)}(z)$ and from the fact that, because of uniform convergence, the integration and the limiting processes can be interchanged.

To prove the uniform convergence of $\{\Psi^{(j)}(z)\}$ for $z \in \Omega$ we shall proceed similarly to the method used on the interval $[0, 1]$. Since the sums (47) are finite, they commute with the integral (43) from the definition of $U_n^{(0)}(z)$ and so

$$\Psi^{(j)}(z) \equiv \sum_{n=0}^j \frac{\varphi_n}{\lambda_n} U_n^{(0)}(z) = \int_0^1 \log(t-z) \sum_{n=0}^j \varphi_n u_n(t) dt. \quad (50)$$

Using arguments similar to those which led to Eq. (35), we find

$$\left| \sum_{j+1}^{j+k} \psi_n U_n^{(0)}(z) \right|^2 \leq \int_0^1 |\log(t-z)|^2 dt \cdot \sum_{j+1}^{j+k} \varphi_n^2 \quad (51)$$

where, for all $z \in \Omega$, the integral over the logarithm is bounded while the sum over the coefficients φ_n^2 tends to zero as j becomes large. This proves the uniform convergence of the sequence $\{\Psi^{(j)}(z)\}$ in Ω and hence, by the theorem of Morera, that the function $\Psi^\infty(z)$ has no singularities in the region Ω .

These results can also be proved using a theorem of Vitali¹³ which states that if: (a) the functions $\Psi^{(j)}(z)$ are holomorphic for $z \in \Omega$, (b) the sequence converges uniformly on some subset Σ of Ω which has an accumulation point inside Ω and (c) the functions $\Psi^{(j)}(z)$ are *uniformly bounded* in Ω , then the functions $\Psi^{(j)}(z)$ tend uniformly towards a function $\Psi^\infty(z)$ which is holomorphic in Ω . Note that the subset Σ may be the segment just above the real interval $[0, 1]$ where the uniform convergence has been proved in Section V A 3.

Using Vitali's theorem we can easily find the regions where $\Psi^\infty(z)$ is holomorphic, by looking at the sets where the $\Psi^{(j)}(z)$ are bounded. In this way we can verify that unlike the functions $U_n^{(0)}(z)$ which can be continued on higher Riemann sheets, the limit $\Psi^\infty(z)$ generally *does not exist* there. This is so because the uniform boundness condition (c) is no longer fulfilled outside the first Riemann sheet (unless the coefficients ψ_n decrease exponentially quickly). The

reason is the existence of the factor $\exp(i\lambda_n(z-t))$ in the higher Riemann sheet continuations $U_n^{(k)}(z)$ of the functions $U_n^{(0)}(z)$ —see Eq. (65) from Section V B 4—which grows exponentially with λ_n if $(z-t)$ is complex.

Finally we shall show that, similar to $\psi^{(\infty)}$ on the real segment, the limit $\Psi^\infty(z)$ coincides inside Ω with the function $\Psi(z)$ defined in Eq. (46). This is a direct consequence of the fact that the set $\ker \mathbf{K}$ is empty in the case of the logarithmic kernel. Indeed, replacing $U_n^{(0)}(z)$ in Eq. (47) by its definition (43), Eq. (46) and the Schwarz inequality give

$$|\Psi(z) - \Psi^{(j)}(z)|^2 \leq \left\| \varphi(x) - \sum_0^j \varphi_n u_n(x) \right\|_{L^2}^2 \int_0^1 |\log(t-z)|^2 dt \quad (52)$$

where the right hand side tends to zero when j grows. [For kernels other than the logarithmic one with non empty null space, we can define appropriate Ψ -functions so that the corresponding φ -functions are contained in $\ker^\perp \mathbf{K}$. The simplest way to do this is to begin with a Neumann series but stop after few iterations so that the new $\varphi(x)$ should belong itself to $\text{Ran } \mathbf{K}$.]

5. Sums of asymptotic expressions

One of the goals of Section V B is to derive asymptotic expressions valid for $z \rightarrow 0$ for the analytic extensions $U_n^{(0)}(z)$ of the eigenfunctions:

$$U_n^{(0)}(z) = U_{n,\text{asy}}^{(0)}(z) + U_{n,\text{rem}}^{(0)}(z). \quad (53)$$

The remainder $U_{n,\text{rem}}^{(0)}(z)$ behaves like $\mathcal{O}(|z|^{k-\eta})$ where k is some given positive integer and $\eta > 0$ but otherwise arbitrary small. However, the coefficients of the asymptotic terms $U_{n,\text{asy}}^{(0)}(z)$ contain some (fixed) positive power of the eigenvalue λ_n , depending on the value of the exponent k . Since the $\{\lambda_n\}$ tend to infinity with n , we should choose carefully an appropriate definition for the $\{\Psi_{\text{asy}}^{(j)}\}$ in order to secure their convergence.

The simplest way to solve this problem is to use the iterated integral equations (10) discussed in Section III. The eigenfunctions of the iterated kernels $K_r(x,t)$ (12) are identical with those of the initial one, the only change being that the eigenvalues are now $(\lambda_n)^r$. This introduces a beneficial factor $1/\lambda_n^r$ in the coefficients $\psi_{r,n}$ of the new functions

$$\psi_r(x) = \int_0^1 K_r(x,t)\varphi(t)dt, \quad (54)$$

which are now

$$\psi_{r,n} = \frac{\varphi_n}{\lambda_n^r}. \quad (55)$$

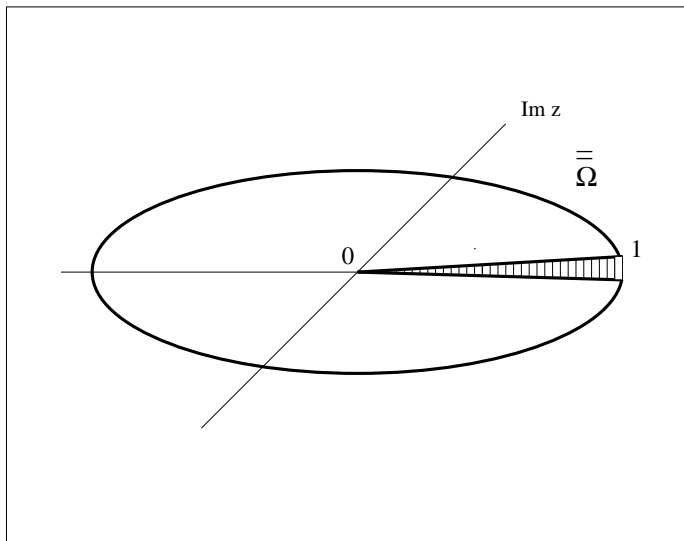


FIG. 7. The closure $\overline{\overline{\Omega}}$ of Ω drawn in three dimensions in order to emphasize that the interval $[0, 1]$ is included twice.

This ensures the separate convergence of the series

$$\Psi_{\text{asy}}^{(j)}(z) = \sum_{n=0}^j \psi_{r,n} U_{n,\text{asy}}^{(0)}(z) = \sum_{n=0}^j \frac{\varphi_n}{\lambda_n^r} U_{n,\text{asy}}^{(0)}(z) \quad (56)$$

and

$$\Psi_{\text{rem}}^{(j)}(z) = \sum_{n=0}^j \psi_{r,n} U_{n,\text{rem}}^{(0)}(z) = \sum_{n=0}^j \frac{\varphi_n}{\lambda_n^r} U_{n,\text{rem}}^{(0)}(z).$$

As a result the asymptotic expansion of the solution of the integral equation will contain terms of the form $z^m \log^k(z)$, $k \leq r$, $m \geq k$, as do the iterated free term [see Eq. (23)] and the asymptotic terms $U_{n,\text{asy}}^{(0)}(z)$.

The initial range of validity of the asymptotic expressions derived above is the cut open disk Ω and so does not yet extend on the real segment $[0, 1]$. We are of course interested to show the correctness of these asymptotic series also on some small real interval $0 \leq x \leq x_0$. As has been shown above, the theorem of Vitali fails to work on higher Riemann sheets since the functions $U_n^{(1)}(z)$ and $U_n^{(-1)}(z)$ are no longer uniformly bounded and so the sequence $\{\Psi^{(j)}(z)\}$ does not converge any more there. However it is interesting and important for what follows to note that the sequence $\{\Psi^{(j)}(z)\}$ related to our integral equation with logarithmic kernel converges uniformly also on the closure $\overline{\overline{\Omega}}$ of Ω , i.e. the function $\Psi^\infty(z)$ is well defined and continuous (because of the uniform convergence) on the real interval $[0, 1]$, both when approached from above and below.

We have used the symbol $\overline{\overline{\Omega}}$ to emphasize the fact that in all this discussion the open set Ω has to be considered as an open subset of the whole Riemann manifold of the solution of the integral equation rather than of the z -complex plane (whereas normally the closure $\overline{\Omega}$ coincides with the unit disk $|z| \leq 1$). The set $\overline{\overline{\Omega}}$ contains the interval $[0, 1]$ twice (see Fig. 7) corresponding to the fact that the function $\Psi(z)$ has different limits when z approaches the interval $[0, 1]$ from above or below.

To prove that the sequence $\{\Psi^{(j)}(z)\}$ converges uniformly also on the interval $[0, 1]$ it is sufficient to note that when $z \in [0, 1]$, $|\log(t - z)|$ is equal to $|\log|t - z||$ if $t > z$, or to $|\log|t - z| \pm i\pi|$ if $t < z$. Here the sign of $i\pi$ depends on whether z approaches the real axis from above or from below. However in both cases the integral from Eq. (52) is bounded and hence, the right hand side of (52) can be made as small as one wishes by taking j to be sufficiently large.

It has been already shown in the previous subsection that limit $\Psi^\infty(z)$ coincides with the holomorphic function $\Psi(z)$ throughout the open set Ω . The limit $\Psi^\infty(z)$ does not exist beyond the two real segments $[0, 1]$ from the border of $\overline{\overline{\Omega}}$ but is continuous up to and on them, because of the uniform convergence of the sequence $\{\Psi^{(j)}(z)\}$. The function $\Psi^\infty(z)$ is hence defined, by continuity, in an unambiguous way on the two real intervals on the boundary of $\overline{\overline{\Omega}}$. It coincides there with $\Psi(z)$, as everywhere else in the closed set $\overline{\overline{\Omega}}$.

In this way we have shown that the asymptotic series $\Psi_{\text{asy}}^\infty(z)$ obtained using the asymptotic expansions of $U_n^{(0)}(z)$ are valid in a neighbourhood of the origin in $\overline{\overline{\Omega}}$, and therefore on the (two) real intervals $[0, x_0]$. This means that the remainder $\Psi_{\text{rem}}^\infty(z)$ of the asymptotic series is bounded by $\mathcal{O}(|z|^{k-\eta})$ on the real interval $[0, x_0]$ as well as in the open set Ω .

B. Continuation of the eigenfunctions to the complex plane

In this subsection we shall study the singularities of the eigenfunctions. To this end, similar to the analytic extension $F^{(0)}$ of the free term from Section IV we shall introduce in Section V B 2 the analytic extensions $U_n^{(0)}$ of the eigenfunctions $u_n(x)$.

In trying to continue $U_n^{(0)}$ analytically on higher Riemann sheets, i.e. in trying to construct the function $U_n^{(1)}$ as we did with the free term in Section IV, we face a specific difficulty related to the fact that the eigenfunctions $u_n(x)$ as they stand, are defined only on the segment $[0, 1]$. This means that we could no longer 'hook' the integration contour, as we did in Section IV where

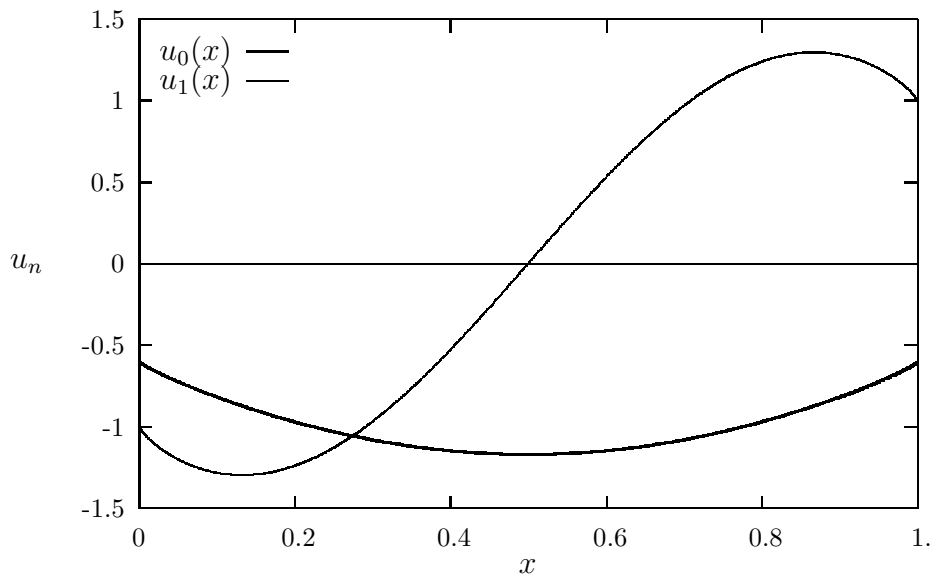


FIG. 8. The eigenfunctions $u_0(x)$ and $u_1(x)$.

the weight $w(t)$, being analytic, was well defined not only on the real segment but also on the various complex plane deformations of the initial integration path.

This point will be solved in Section *V B 3* where the eigenfunctions $u_n(x)$ will be expressed as linear combinations of $U_n^{(0)}$ and its Riemann sheet continuations. Another consequence of this fact will be the Volterra integral equation which relates $U_n^{(1)}$ to $U_n^{(0)}$ or vice versa (Section *V B 4*). This Volterra integral equation can be solved effectively, providing explicit expressions for $U_n^{(1)}$ or $U_n^{(-1)}$ in terms of $U_n^{(0)}$. Finally, in Section *V B 5* this integral equation is used in order to derive the asymptotic series which describe the singularities of the eigenfunctions around the origin.

1. Eigenfunctions of the logarithmic kernel

It has been proved in the Section *V A 3* that, in spite of the logarithmic singularity in the integrand, the eigenfunctions $\{u_n\}$ defined by

$$u_n(x) = \lambda_n \int_0^1 \log |t - x| u_n(t) dt \quad (57)$$

are continuous functions. The graphs of some of these eigenfunctions are depicted in Fig. 8 and Fig. 9. Although these eigenfunctions are finite and look well behaved at the end points 0 and 1 of the fundamental domain (they are there continuous), their derivatives are there infinite. It

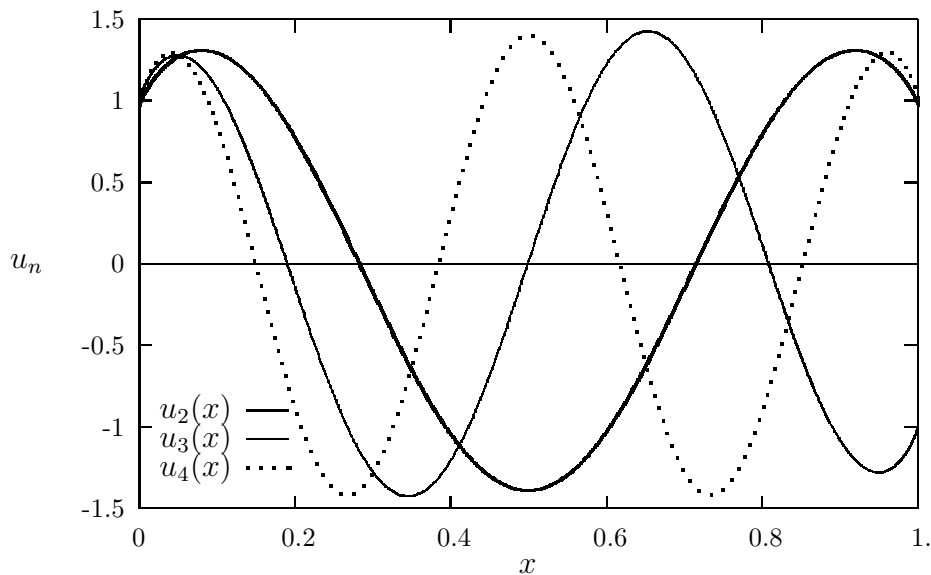


FIG. 9. The eigenfunctions $u_2(x)$, $u_3(x)$ and $u_4(x)$.

is the aim of the following subsections to give a full analytic description of the singularities of $u_n(x)$ at these end points.

Notice that initially, in order to compute the eigenfunctions $u_n(x)$ it has been sufficient to take the range of the variable x to be the same as that of the integration variable t . Usually to compute the function from the left hand side of an integral equation for values of the variable x outside this initial range, we take the so-called Nyström continuation, which consists simply of substituting the new values of x in the right hand side of the equation. However this is possible *only* if the kernel is holomorphic in some given region and so this method is not applicable in our case because of the modulus function inside the logarithm which spoils holomorphy. Thus if in Eq. (57) we take x to be negative, the left hand side " $u_n(x)$ " is *not* the analytic continuation of the function $u_n(t)$ which appears on the right hand side.

2. The functions $U_n^{(0)}(z)$ and their analytic continuations $U_n^{(\pm k)}(z)$

The function " $u_n(x)$ " which was defined in this naive way for negative values of x , may be used to introduce a new function $U_n^{(0)}(z)$ which is analytic and, although different from $u_n(x)$ when $x \in [0, 1]$, is intimately related to it. Noticing that for $x < 0$ and $\forall t \in [0, 1]$ we have

$\log|t-x| = \log(t-x)$, we shall define $U_n^{(0)}(z)$ by

$$U_n^{(0)}(z) \stackrel{\text{def}}{=} \lambda_n \int_0^1 \log(t-z) u_n(t) dt, \quad n = 1, 2, 3, \dots \quad (58)$$

Taking the cut of $\log(Z) \equiv \log(t-z)$ along the real negative axis of the complex $Z \equiv t-z$ -plane, $U_n^{(0)}(z)$ is a complex function of real type, $U_n^{(0)}(z) = \overline{U_n^{(0)}(\bar{z})}$, having, as we shall show later, a branch point at the origin and a cut lying on the positive real axis. Since we are interested in the singularity of the function near the origin we shall consider the detailed behaviour of $U_n^{(0)}(z)$ only in the neighbourhood of $z = 0$. A similar analysis can be performed at the point $z = 1$.

The superscript $(^{(0)})$ in the present case) of $U_n^{(k)}(z)$ denotes the Riemann sheet under consideration. Our notation will be such that, by crossing the cut of $U_n^{(k)}$ between $z = 0$ and $z = 1$ in an *anti-clockwise* way, the value of the superscript increases by 1: see, in Fig. 10, the full line $\alpha^{(0)}-\beta^{(0)}$ from the sheet (0), which is continued by the dashed-line $\alpha^{(1)}$ lying on sheet (1). Conversely, crossing the cut between 0 and 1 in the *clockwise* direction, we pass from the full line $\alpha^{(0)}$ from the sheet (0) to the dotted-line $\beta^{(-1)}$ from the sheet (-1) .

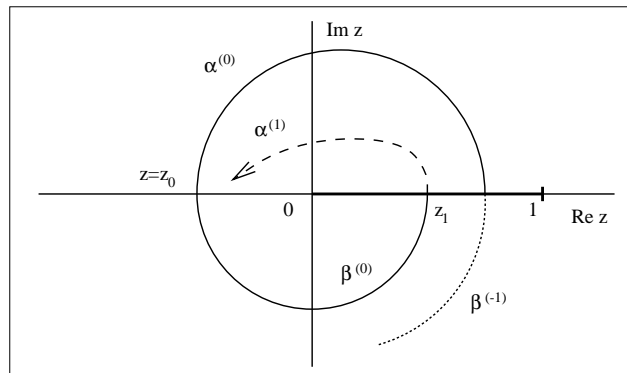


FIG. 10. Higher Riemann sheet continuations of $U_n^{(0)}$.

We will want to continue the function $U_n^{(0)}(z)$ defined by the right hand side integral from Eq. (58), starting from some point $z = z_0$ ($z_0 < 0$), along the full-line path $\beta^{(0)}$ and the dashed-line $\alpha^{(1)}$, back to z_0 , obtaining in this way the value $U_n^{(1)}(z_0)$ of $U_n(z)$ on the next Riemann sheet. But in so doing we will need to deform the integration contour on the right hand side of Eq. (58) into the upper half complex t -plane as we did in the case of the free term in Section IV. We are faced, however, with the difficulty that $u_n(t)$, as it stands, is defined only on the real segment $0 \leq t \leq 1$. We therefore need to express $u_n(t)$ as the value of some analytic function on the upper edge of the cut. Here we will be interested only in *the upper lip* of the cut, since moving in an anti-clockwise direction, the analytic continuation path will hook and deform the integration contour into the *upper half* of the complex t -plane (see the curve C from Fig. 5).

3. Expressing $u_n(t)$, $0 < t < 1$, in terms of $U_n^{(0)}(t + i\varepsilon)$ and $U_n^{(1)}(t + i\varepsilon)$

Our first concern will be to rewrite the functions appearing under the integral sign of Eq. (58) as combinations of analytic functions. To this end we again use the definition (58) and start from some point $z = z_0$, $z_0 < 0$. We first continue $U_n^{(0)}(z)$ along a path lying in the lower half z -plane to a point $z_- = z_1 - i\varepsilon$, $0 < z_1 < 1$, $\varepsilon > 0$, below the segment $[0, 1]$ (along the path $\beta^{(0)}$ from Fig. 10). If the cut of $\log(Z) \equiv \log(t - z)$ is taken to run along the negative real Z -axis, we have

$$\lim_{\varepsilon \searrow 0} \log(t - (z_1 - i\varepsilon)) = \begin{cases} \log|t - z_1| + i\pi & \text{if } t < z_1, \\ \log|t - z_1| & \text{if } t > z_1. \end{cases}$$

We now split the integral along the segment $[0, 1]$ into one between 0 and z_1 (where, of course, $t < z_1$ and so the integral runs along the upper lip of the cut of the logarithm), and a second one, between z_1 and 1, where the integration points stay apart from the cut of the logarithm. In this way we get

$$\begin{aligned} U_n^{(0)}(z_1 - i\varepsilon) &= \lambda_n \int_0^{z_1} \log|t - z_1| u_n(t) dt + \pi i \lambda_n \int_0^{z_1} u_n(t) dt + \lambda_n \int_{z_1}^1 \log|t - z_1| u_n(t) dt \\ &= u_n(z_1) + \pi i \lambda_n \int_0^{z_1} u_n(t) dt \end{aligned} \quad (59)$$

where the last equality follows simply from the fact that the first and the third terms combine to give exactly the right hand side of Eq. (57).

Similarly we can make an analytic continuation from $z = z_0 < 0$ (along the path $\alpha^{(0)}$ from Fig. 10) to the point $z_+ = z_1 + i\varepsilon$ above the cut, to obtain:

$$\begin{aligned} U_n^{(0)}(z_1 + i\varepsilon) &= \lambda_n \int_0^{z_1} \log|t - z_1| u_n(t) dt - \pi i \lambda_n \int_0^{z_1} u_n(t) dt + \lambda_n \int_{z_1}^1 \log|t - z_1| u_n(t) dt \\ &= u_n(z_1) - \pi i \lambda_n \int_0^{z_1} u_n(t) dt. \end{aligned} \quad (60)$$

The integral over $u_n(t)$ can be eliminated between Eqs. (59) and (60) by taking the sum of the right hand sides, so that

$$\begin{aligned} u_n(z_1) &= \frac{1}{2} [U_n^{(0)}(z_1 + i\varepsilon) + U_n^{(0)}(z_1 - i\varepsilon)] + \mathcal{O}(\varepsilon) \\ &= \frac{1}{2} [U_n^{(0)}(z_1 + i\varepsilon) + U_n^{(1)}(z_1 + i\varepsilon)] + \mathcal{O}(\varepsilon). \end{aligned} \quad (61)$$

Here the last line of Eq. (61) follows from the fact that the values of $U_n^{(1)}$ of the function U_n on the next Riemann sheet on the *upper lip* of the cut, merge, by definition (see also Eq. (17)), with those of $U_n^{(0)}$ *below* the cut:

$$U_n^{(0)}(z_1 - i\varepsilon) = U_n^{(1)}(z_1 + i\varepsilon) + \mathcal{O}(\varepsilon) \quad , \quad 0 < z_1 < 1.$$

4. A Volterra equation for $U_n^{(1)}(z)$

We shall now be able to deform the integration contour in the complex t -plane in the same way as we did in section IV. Recalling that by the analytic continuation of $U_n^{(0)}(z)$ along the path $\beta^{(0)} - \alpha^{(1)}$ from Fig. 10 one obtains the function $U_n^{(1)}(z)$, we find

$$U_n^{(1)}(z_0) = \lambda_n \int_C \log(t - z_0) \frac{U_n^{(0)}(t) + U_n^{(1)}(t)}{2} dt \quad (62)$$

where the integration contour C is shown in Fig. 5 and where we have replaced $u_n(t)$ under the integrand by its holomorphic expression (61). The dashed line represents the cut of $\log(t - z_0)$ in the complex t -plane, where, again, the $+i\pi$ -zone and $-i\pi$ -zone mean that the logarithm differs there by $+i\pi$ and $-i\pi$ with respect to its mean value across the cut. In the region $\text{Re } t < 0$, both $U_n^{(0)}$ and $U_n^{(1)}$ are holomorphic. So—recollect the discussion from section IV which led to Eq. (14)—the integral over the $\text{Re } t < 0$ half-plane part of the contour C yields

$$-i\pi\lambda_n \int_{z_0}^0 [U_n^{(0)}(t) + U_n^{(1)}(t)] dt,$$

while the rest of the integral, between $t = 0$ and $t = 1$, is identical with that from definition (58) of the function $U_n^{(0)}(z_0)$. So, Eq. (62) can be rewritten in the form

$$U_n^{(1)}(z) = U_n^{(0)}(z) + i\pi\lambda_n \int_0^z [U_n^{(0)}(t) + U_n^{(1)}(t)] dt \quad (63)$$

which is valid for any z in the cut complex plane since it involves only analytic expressions. Equation (63) can be regarded as a Volterra integral equation for $U_n^{(1)}(z)$ if the function $U_n^{(0)}(z)$ is known, or equally, as a Volterra integral equation for $U_n^{(0)}(z)$ if $U_n^{(1)}(z)$ were known.

This equation can be solved by differentiation. We find immediately

$$\frac{dU_n^{(1)}(z)}{dz} - \frac{dU_n^{(0)}(z)}{dz} = +i\pi\lambda_n [U_n^{(0)}(z) + U_n^{(1)}(z)], \quad (64)$$

or, rearranging the terms,

$$\frac{dU_n^{(1)}(z)}{dz} - i\pi\lambda_n U_n^{(1)}(z) = \frac{dU_n^{(0)}(z)}{dz} + i\pi\lambda_n U_n^{(0)}(z).$$

This can be rewritten in the form

$$\exp(+i\pi\lambda_n z) \frac{d}{dz} [\exp(-i\pi\lambda_n z) U_n^{(1)}(z)] = \exp(-i\pi\lambda_n z) \frac{d}{dz} [\exp(+i\pi\lambda_n z) U_n^{(0)}(z)].$$

Now, from Eq. (63) it is obvious that $U_n^{(1)}(0) = U_n^{(0)}(0)$. This is an initial condition which permits us to write the solution of the Volterra equation as

$$U_n^{(1)}(z) = U_n^{(0)}(z) + 2i\pi\lambda_n \int_0^z \exp[i\pi\lambda_n(z-t)]U_n^{(0)}(t)dt. \quad (65)$$

Similarly we can step backwards and express $U_n^{(0)}$ with respect to $U_n^{(1)}$, or $U_n^{(-1)}$ with respect to $U_n^{(0)}$:

$$U_n^{(-1)}(z) = U_n^{(0)}(z) - 2i\pi\lambda_n \int_0^z \exp[-i\pi\lambda_n(z-t)]U_n^{(0)}(t)dt. \quad (66)$$

5. Asymptotic expansion

To begin with, we shall suppose that each of the functions $U_n^{(0)}(z)$ admits an expansion around the origin of the form

$$\begin{aligned} U_n^{(0)}(z) &= U_{n,\text{asy}}^{(0)}(z) + U_{n,\text{rem}}^{(0)}(z), \\ &\equiv \sum_{k=0}^r a_k z^k + \sum_{m=1}^r \sum_{k=1}^r b_{mk} z^m \cdot \log^k(-z) + U_{n,\text{rem}}^{(0)}(z) \end{aligned} \quad (67)$$

where $U_{n,\text{rem}}^{(0)}$ is $\mathcal{O}(|z|^{r+1-\eta})$. The choice of these series may look very restrictive, but once we have shown their consistency, their uniqueness follows from the uniqueness of the solution of a linear integral equation with a Hilbert–Schmidt kernel. In Eq. (67) the sum $\sum_{k=0}^r a_k z^k$ comes from the holomorphic part of $U_n^{(0)}$ around $z = 0$. Taking as before the cut of $\log(Z) \equiv \log(-z)$ along the negative real Z -axis, the right hand side of Eq. (67) will be holomorphic throughout the domain Ω which has a cut running along the positive real axis (see Fig. 6). From the definition (58) we see that $U_n^{(0)}(z)$ is a real-analytic function [i.e. $U_n^{(0)}(z) = \overline{U_n^{(0)}(\bar{z})}$] and so the coefficients a_k ($k = 0, 1, 2, \dots$) and b_{mk} ($m, k = 1, 2, \dots$) have to be real. The coefficients b_{mk} are then determined in a recursive manner from the coefficients a_k of the regular part.

In order to find the coefficients b_{mk} we first notice that the analytic continuation of $U_{n,\text{asy}}^{(0)}$ across the cut yields

$$U_{n,\text{asy}}^{(1)}(z) = \sum_{k=0}^r a_k z^k + \sum_{m=1}^r \sum_{k=1}^r b_{mk} z^m \cdot [\log(-z) + 2i\pi]^k. \quad (68)$$

Inserting the expressions (67) and (68) in Eq. (64) we may then compare the various terms appearing in the left and right hand sides. This comparison can be done for any z in the open set Ω , for instance for negative real z , in order to be away from the cut of $\log(-z)$. Taking the limit $z \rightarrow 0$ in both sides we remark that

$$b_{1k} = 0, \quad k = 2, 3, \dots, \quad (69)$$

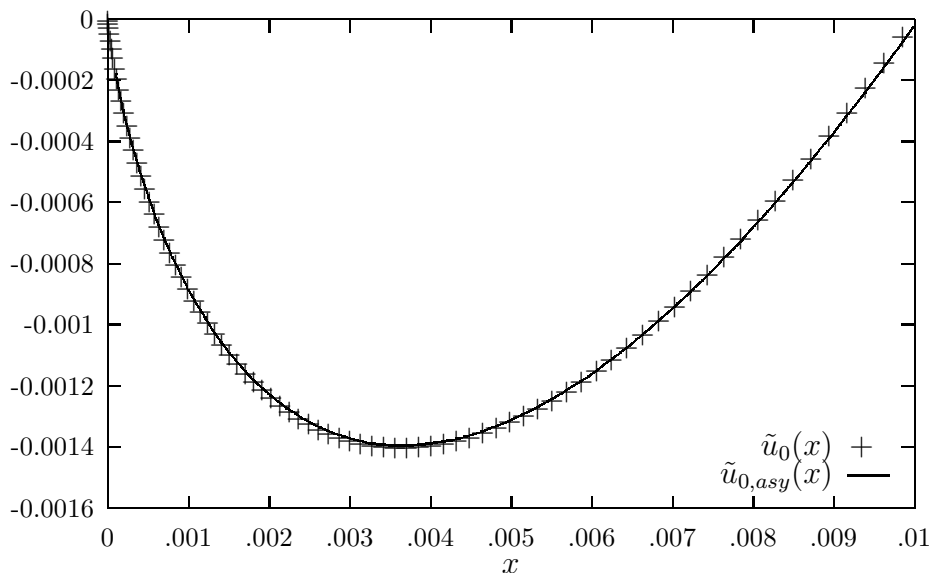


FIG.11. One parameter asymptotic fit of $\tilde{u}_0(x)$.

as a consequence of the fact that the differences of terms of the type $z[\log(-z) + 2i\pi]^k$ and $z \log^k(-z)$ from the left hand side of Eq. (64) yield, by differentiation, terms which tend to infinity and which are not compensated by similar terms from the right hand side. Looking at the constant terms we get

$$b_{11} = \lambda_n a_0. \quad (70)$$

Similarly, by differentiating with respect to z both sides of Eq. (64) we obtain

$$b_{mk} = 0 \quad \text{if } k \geq m + 1, \quad (71)$$

while the coefficients b_{mk} with $k \leq m$ can be expressed iteratively by means of the coefficients a_k . So, for instance, we find

$$b_{21} = \frac{2a_1\lambda_n - a_0\lambda_n^2}{4}, \quad b_{22} = \frac{a_0\lambda_n^2}{4}. \quad (72)$$

We tried to check numerically the accuracy of this asymptotic expansion in regions close to the singularity. To this end we took two terms from the holomorphic part of $U_{n,\text{asy}}^{(0)}(z)$, and expressed the corresponding b_{mk} coefficients in terms of the first two coefficients a_0 and a_1 . Since a_0 is determined by the value at $x = 0$ of the eigenfunctions which, in turn, is determined by the normalization condition, we have in fact *only one free parameter*, the coefficient a_1 . Using

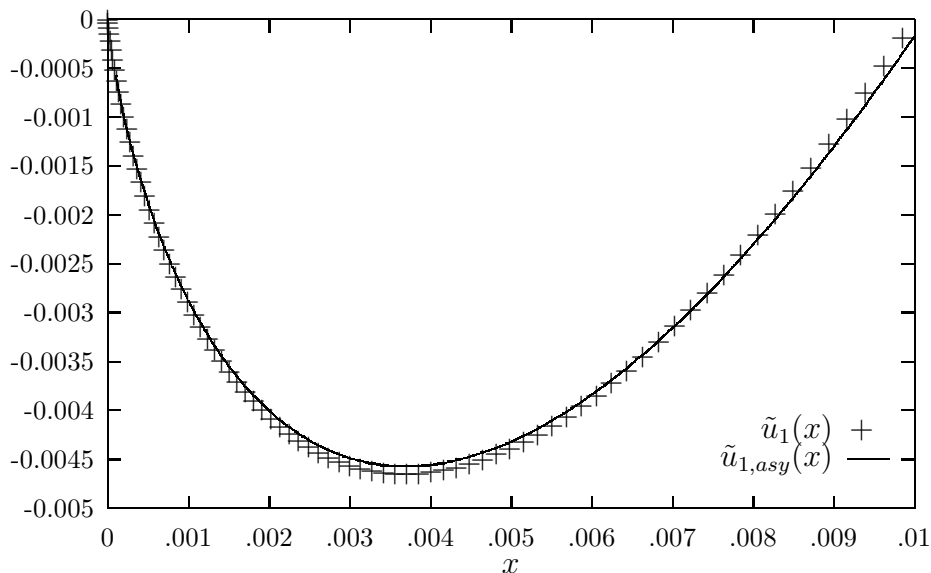


FIG.12. One parameter asymptotic fit of $\tilde{u}_1(x)$.

the above expressions for b_{11} , b_{21} and b_{22} in terms of a_0 (given) and a_1 (free), we have chosen a_1 to obtain the best fit to the first few eigenfunctions, in the region $[0, 0.01]$ near the origin where we expected the asymptotic expansion to hold. When we plot the function $u_n(x)$ together with our asymptotic expansion the two curves appear identical on the interval $[0, 0.01]$. In order to show the slight difference in these functions we have defined a new function $\tilde{u}_n(x) = u_n(x) - u_n(0) - (u_n(x_1) - u_n(0))x/x_1$ which has its end points $\tilde{u}_n(0)$ and $\tilde{u}_n(0.01)$ at the same height and so permits the use of a much enlarged y -axis scale. The corresponding plots for the two first eigenfunctions are presented in Figs. 11 and 12. Although as it has been already stressed, these curves are just one parameter fits and that moreover we have restricted ourselves only to the first terms in the asymptotic expression, the agreement between these asymptotic expressions (the full lines) with the computer calculated points of the eigenfunctions (the crosses) is really excellent.

VI. RESUME AND CONCLUSIONS

As indicated in the Introduction, the numerical calculations related to the solution of the inverse problem for EIT are seriously hampered by the high number of mesh points necessary to take into account the sharp peaks of the current density near the edge of the electrodes. Since these peaks seemed to be intrinsic objects describable by only a small numbers of parameters we

have investigated the details of their analytic structure. To this end we have studied the Riemann sheet structure of the eigenfunctions of the dominant singular integral equation relating to the solution of the mixed boundary problem for the potential, and derived asymptotic expressions both for the eigenfunctions and for the solution of the integral equation. These asymptotic expressions provide very simple parametrisations for the anomalous thresholds, whose effectiveness can be judged from the Figs. 11 and 12.

The paper is constructed as follows: In the Introduction and in Section II the mathematics of the EIT modelling is discussed while the corresponding weakly singular integral equation is given in Section III. In Section IV we have discussed the effect on the singularities of the free term of the moving cut of the logarithm which 'hooks' the integration contour. The *generic singularities* of the solution of the integral equation are then described as a superposition of those of the free term and of the eigenfunctions which were derived in Section V B. Section V A contains the proof that although we deal with infinite series, no new singularities appear in the neighbourhood of the origin, i.e. the singularities of the solution are really those of the eigenfunctions and of the free term. We also determine the limits of the domain where the eigenfunction sum converges unconditionally and show how one can extend the validity of the asymptotic series also on the real segment $[0, 1]$.

We hope that the discussion of the analytic properties of the eigenfunctions and solution of this quite special, logarithmic singular equation, will provide a working example which might be useful also for the study of the singularities of the solution of other weakly singular integral equations. The discontinuities across the cuts will certainly be different, but the general discussion will probably be fairly similar.

ACKNOWLEDGEMENTS

The authors are grateful to Professors G. Auberson, G. Mennessier and P. C. Sabatier for long discussions concerning the integral equation and other analytic aspects of this paper. One of authors (M.K.P.) would like to thank The British Council for its support. Another author (S.I.) acknowledges a research grant from the Ministère de l'Enseignement Supérieur et de la Recherche and the help of Professor C. Duhamel from the French Embassy in Bucharest without whom this collaboration would not have been possible.

APPENDIX: COMPLETENESS OF THE BASIS $\{u_n\}$

Following a proof given by G. Auberson,¹⁴ we shall show in what follows that $\ker \mathbf{K}$, the null space of the logarithmic kernel, is empty and so the eigenfunctions $\{u_n\}_{n=0,1,2,\dots}$ do span the whole Hilbert space of the L^2 functions on $[0, 1]$.

Suppose that $\ker \mathbf{K} \neq \{0\}$, i.e. that there exists at least one non zero L^2 -function ϕ such that

$$\int_0^1 \log|x-y| \phi(y) dy = 0. \quad (\text{A1})$$

Defining the function

$$v(x) \stackrel{\text{def}}{=} \int_0^x \phi(y) dy, \quad (\text{A2})$$

we have

$$\begin{aligned} a) \quad & \frac{dv(x)}{dx} = \phi(x) \quad \text{almost everywhere,} \\ b) \quad & v(0) = 0. \end{aligned}$$

We can easily prove that the function $v(x)$ satisfies a Hölder condition of index $1/2$

$$|v(x_1) - v(x_2)| \leq A |x_1 - x_2|^{1/2}, \quad \text{for } \forall x_1, x_2 \in (0, 1),$$

where A is a positive constant.

By integrating the left hand side of Eq. (A1) by parts we find

$$\int_0^1 \log|x-y| \phi(y) dy = v(1) \log(1-x) - \mathcal{P} \int_0^1 \frac{v(y)}{y-x} dy$$

so that from Eq. (A1) we obtain

$$\mathcal{P} \int_0^1 \frac{v(y)}{y-x} dy = v(1) \log(1-x), \quad (\text{A3})$$

If we now consider the following function

$$F(z) \stackrel{\text{def}}{=} \sqrt{z(z-1)} \int_0^1 \frac{v(y)}{y-z} dy \quad \text{for } z \in D \quad (\text{A4})$$

where D is the complex z -plane cut along the segment $[0, 1]$, we can show that:

- (i) F is a holomorphic function in D ;
- (ii) $\lim_{z \rightarrow \infty} F(z) = -\int_0^1 v(y) dy$;
- (iii) $\text{Im } F(x + i\varepsilon) = \sqrt{x(1-x)} \mathcal{P} \int_0^1 \frac{v(y)}{y-x} dy = \sqrt{x(1-x)} v(1) \log(1-x)$, for $x \in (0, 1)$;
- (iv) $\text{Re } F(x + i\varepsilon) = -\pi \sqrt{x(1-x)} v(x)$, for $x \in (0, 1)$.

The properties (i) – (iii) imply that

$$F(z) = \frac{v(1)}{\pi} \int_0^1 \frac{\sqrt{y(1-y)} \log(1-y)}{y-z} dy - \int_0^1 v(y) dy, \quad z \in D, \quad (\text{A5})$$

while from (iv) it follows that for $x \in (0, 1)$ we have

$$-\pi \sqrt{x(1-x)} v(x) = \frac{v(1)}{\pi} \mathcal{P} \int_0^1 \frac{\sqrt{y(1-y)} \log(1-y)}{y-x} dy - \int_0^1 v(y) dy. \quad (\text{A6})$$

Taking now the limits $x \searrow 0$ and $x \nearrow 1$ we find

$$\frac{v(1)}{\pi} \int_0^1 \sqrt{\frac{1-y}{y}} \log(1-y) dy - \int_0^1 v(y) dy = 0, \quad (\text{A7})$$

$$-\frac{v(1)}{\pi} \int_0^1 \sqrt{\frac{y}{1-y}} \log(1-y) dy - \int_0^1 v(y) dy = 0. \quad (\text{A8})$$

Subtracting (A8) from (A7) we see that $v(1) = 0$ and hence, from Eq. (A6),

$$v(x) = \frac{1}{\pi \sqrt{x(1-x)}} \int_0^1 v(y) dy \equiv \frac{C}{\pi \sqrt{x(1-x)}}. \quad (\text{A9})$$

Now, since $v(1)$ is zero, the constant C has to be zero too and so $v(x)$ has to vanish identically [it had to be so since neither the right hand side of Eq. (A9) and even less its derivative are L^2]. This implies that $\ker \mathbf{K}$ is an empty set and so the eigenfunctions $\{u_n\}$ of the logarithmic kernel form a complete L^2 basis on the segment $[0, 1]$.

¹ See for example the collection of papers in *Physiol. Meas.*, **16**, Supplement **3A**, (1995).

² K.S. Paulson, W.R. Breckon and M.K. Pidcock, 'Electrode modelling in Electrical Impedance Tomography', *SIAM J. Appl. Math.*, **52**, pp. 1012–1022, (1992).

³ E. Sommersalo, M. Cheney and D. Isaacson, 'Existence and uniqueness for electrode models for Electric Current Computed Tomography', *SIAM J. Appl. Math.*, **52**, pp. 1023–1041, (1992).

⁴ M.K. Pidcock, S. Ciulli and S. Ispas, 'Singularities of mixed boundary value problems in Electrical Impedance Tomography', *Physiol. Meas.*, **16**, pp. 213–218, (1995).

⁵ K. Cheng, D. Isaacson, J.C. Newell and D.G. Gisser, 'Electrode models for electric current computed tomography', *IEEE Trans. Biomed. Engrg.*, **36**, pp. 918–924, (1989).

⁶ S. Ciulli, S. Ispas and M.K. Pidcock, 'Numerical modelling of a mixed Neumann–Robin boundary value problem', PM–95/22, submitted for publication (1996).

- ⁷ R.J. Eden, P.V. Landshoff, D.I. Olive and J.C. Polkinghorne, *The analytic S-matrix*, (Cambridge University, Cambridge, 1966).
- ⁸ see for instance M. Ciulli, S. Ciulli and T.D. Spearman, 'Bounds for the Continuation of Perturbative Results in the Spectral Region', *J. Math. Phys.* **25**, pp. 3194–3203, (1984).
- ⁹ F.D. Gakhov, *Boundary Value Problems*, (Pergamon, London, 1966).
- ¹⁰ S. Ciulli, S. Ispas and M.K. Pidcock — 'Riemann sheet structure of eigenfunctions for a boundary value problem related to Electrical Impedance Tomography', in preparation (1996).
- ¹¹ W. Rudin, *Real and Complex Analysis*, (McGraw–Hill, New York, 1970).
- ¹² J. W. Dettmann, *Applied Complex Variables*, (MacMillan, New York, 1965).
- ¹³ E. C. Titchmarsh, *The Theory of Functions* 2nd ed. (Oxford University Press, London, 1939).
- ¹⁴ G. Auberson, private communication.